https://doi.org/10.5194/egusphere-2022-1060
Preprint. Discussion started: 26 October 2022

Including ash in UKESM1 model simulations of the Raikoke volcanic eruption reveal improved agreement with observations

Alice F. Wells[1], Andy Jones[2], Martin Osborne[2], Lilly Damany-Pearce[1], Daniel G. Partridge[1] and James M. Haywood[1,2]

[1]Department of Mathematics, University of Exeter, Exeter, EX4 4QE, United Kingdom
[2]Met Office, Exeter, EX1 3PB, United Kingdom

Correspondence to: Alice F. Wells (afw207@exeter.ac.uk)

Abstract. In June 2019 the Raikoke volcano located in the Kuril Islands, northeast of Japan, erupted explosively and emitted approximately 1.5Tg ± 0.2 Tg of SO_2 and 0.4 – 1.8 Tg of ash into the upper troposphere and lower stratosphere. Volcanic ash is usually neglected in modelling stratospheric climate changes since larger particles have generally been considered to be short-lived in terms of their stratospheric lifetime. However, recent studies have shown that the coagulation of mixed particles with ash and sulfate is necessary to model the evolution of aerosol size distribution more accurately. We perform simulations using a nudged version of the UK Earth System Model (UKESM1) that includes a detailed 2-moment aerosol microphysical scheme for modelling the oxidation of sulfur dioxide (SO_2) to sulfate aerosol and the detailed evolution of aerosol microphysics in the stratosphere. We compare the model with a wide range of observational data. The current observational network including satellites and surface based lidars and high-altitude sun-photometers means that smaller-scale eruptions such as Raikoke provide unprecedented detail of the evolution of volcanic plumes and processes, but there are significant differences in the evolution of the plume detected using the various satellite retrievals. These differences stem from fundamental differences in detection methods between e.g. lidar and limb-sounding measurement techniques and the associated differences in detection limits and the geographical areas where robust retrievals are possible. This study highlights that, despite the problems in developing robust and consistent observational constraints, the balance of evidence suggests that including ash in the model emission scheme provides a more accurate simulation of the evolution of the volcanic plume within UKESM1.

1 Introduction

Throughout history large explosive volcanic eruptions have resulted in periodic perturbations to the climate. Explosive volcanic eruptions frequently emit a combination of gases, including sulfur dioxide (SO_2) and volcanic ash into the UTLS (Upper Troposphere-Lower Stratosphere) where the SO_2 oxidises resulting in the formation of secondary sulfate aerosols. Sulfate aerosols in the stratosphere have a residence time of several months to a few years (e.g. Robock, 2000; Langmann, 2014; Jones et al., 2017) due to limited wet and dry deposition rates (Kloss et al., 2021). Sulfate aerosols are primarily reflective and enhance the scattering of shortwave solar radiation, increasing the albedo of the planet and thus exert a cooling effect on the Earth's climate system (e.g., Robock, 2000; Gordeev, 2014). The extent of their impact upon the climate is dependent on

https://doi.org/10.5194/egusphere-2022-1060
Preprint. Discussion started: 26 October 2022

a multitude of parameters, including the magnitude of the emission, location of the volcano, the injection altitude, and the composition of the plume (e.g. Jones et al., 2017).

In June 1991 Mount Pinatubo injected an estimated 10-20 Tg of SO_2 into the lower stratosphere (Bluth et al., 1992; Dhomse et al., 2014) causing potentially the largest aerosol perturbation to the stratosphere in the 20th century and resulting in average lower tropospheric global temperatures cooling by around 0.5°C across a period of nearly two years (McCormick et al., 1995; Guo et al., 2004). Whilst there has not been another volcanic eruption since Pinatubo to have such a significant impact on the global climate in subsequent years, there have been a series of more moderate eruption. Kasatochi in Alaska erupted in August 2008, injecting an estimated 1.4 – 1.6 Tg of SO_2 (Kravitz et al., 2010; Karagulian et al., 2010). The following year in June 2009, Sarychev Peak on the Kuril Islands was estimated to have injected 1.2 $\pm$ 0.2 Tg (Haywood et al., 2010) and in June 2011 Nabro in Eritrea erupted injecting around 1.3 – 1.5 Tg of SO_2 (Clarisse et al., 2012). Haywood et al., (2014) estimate that over the period 2008 – 2012 these smaller volcanic eruptions contributed to between -0.02 and -0.03 K of cooling at the Earth's surface.

While these volcanic eruptions injected an order of magnitude less SO_2 into the stratosphere than Pinatubo, monitoring the transport, evolution and dispersion of volcanic plumes allows an assessment of the performance of global climate models in representing stratospheric sulfate plumes, and allows improvements to be made in key processes. The much-improved observational network compared to that which observed the Pinatubo eruption, which includes satellite observations of both SO_2 (e.g. Cai et al., 2022) and sulfate aerosol (REFS), surface based lidars (e.g. Chouza et al., 2020), high-altitude sun-photometers (e.g. Toledano et al., 2018), and periodic balloon-borne observations (e.g. Jégou et al., 2013) means that observations of these smaller-scale eruptions provide unprecedented detail of the evolution of volcanic plumes and processes. The validation and improvement of representation of volcanic plumes within global climate models leads to a better understanding of their associated cooling impacts. Such synergy between observations and models also provides a means to assess the uncertainties associated with proposed stratospheric aerosol injection climate intervention strategies that have recently been suggested as a method to ameliorate the worst impacts of climate change (e.g. Lawrence et al., 2018).

This study examines the impact of the 2019 eruption of Raikoke. Almost exactly a decade after the eruption of Sarychev Peak (12th June 2009, 48.1°N, 153.2°E) on 21st June 2019 at 1800 UTC, a neighbouring volcano – Raikoke (48.3°N, 153.2°E) – started to erupt, generating a series of distinct explosive events, and emitting a plume of ash and SO_2 into the stratosphere. During this period, it is estimated that it injected around 1.5 $\pm$ 0.2 Tg of SO_2 (Muser et al., 2020; Kloss et al., 2021; De Leeuw et al., 2021) and 0.4 – 1.8 Tg of ash (Bruckert et al., 2022) into the stratosphere signifying the largest volcanic emission of SO_2 since the Nabro eruption in 2011. The resultant volcanic aerosol plume was detected at altitudes ranging between 11 to 20km by the TROPOMI instrument (Hedelt et al., 2019; Vaughan et al., 2020) and at similar altitudes by other satellite instruments (e.g., Gorkavyi et al., 2021, Kloss et al., 2021), although altitudes as high as 26km have been inferred in isolated lidar

https://doi.org/10.5194/egusphere-2022-1060
Preprint. Discussion started: 26 October 2022

measurements (e.g. Chouza et al., 2020). These findings indicate that a significant portion of the volcanic plume was injected into the stratosphere. Gorkavyi et al. (2021) found that the peak sulfate aerosol extinction occurred around 1.5 months after the eruption date with an SO_2 e-folding lifetime of approximately 19 days. Previous studies looking at similar volcanic eruptions have found SO_2 *e*-folding times at a similar scale. For example, once the retrieval minimum detection threshold had been accounted for, Haywood et al., 2010 determined an e-folding for SO_2 from the Infrared Atmospheric Sounding Interferometer (IASI) for the Sarychev Peak eruption of around 20-22 days.

Less than a week after the eruption of Raikoke a second volcanic eruption occurred – Ulawun (5.1°S, 151.3°E) – on 26th June 2019 and again on 3rd August 2019. It is estimated to have injected around 0.14 Tg SO_2 into the stratosphere during the first explosive eruptive phase and a further 0.2 Tg SO_2 during the second phase of the eruption (Kloss et al., 2021).

The Raikoke and Ulawun eruptions were both well observed by a series of satellite instruments and ground-based measurement stations. Satellite observations include the Ozone Mapping Profiler Suite (OMPS) Nadir Mapper (NM) (Yang, 2017) and Limb Profiler (LP) (Taha, 2020) and the Cloud-Aerosol Lidar with Orthogonal Polarization (CALIOP) (Winker et al., 2009) while surface observations include those from high altitude AErosol RObotic NETwork sites (AERONET; Holben et al., 1998). Although the perturbations to the Earth's radiation budget and near-surface temperature from moderate volcanic eruptions, such as Raikoke, are unlikely to be detectable owing to the small signal-noise ratio, these impacts can be estimated from Earth System models. The Raikoke eruption was the largest volcanic stratospheric injection of SO_2 since the OMPS satellite was launched in late 2011 providing an excellent opportunity to assess the skill and the limitations of the UK Earth System Model (UKESM1; Sellar et al., 2019) in simulating the evolution of the atmospheric distributions of SO_2 and sulfate aerosol.

Recent studies have drawn attention to the influence of ash on self-lofting and the evolution of the volcanic plume (e.g., Muser et al., 2020; Kloss et al., 2021). Volcanic ash is usually neglected in the modelling the impact of eruptions on the stratosphere and climate since larger particles would be short lived owing to their considerable fall-speed (Niemeier et al., 2009). However, Zhu et al., 2020 showed that, to produce the evolution of the size distribution following the Kelud eruption in 2014, the coagulation of internally mixed ash and sulfate particles is necessary. They also found that after this eruption ash particles were the main component of the volcanic aerosol layer. Including ash emissions in model simulations can alter the dynamics of sulfate aerosol formation (Shallcross et al., 2021) including prolonging the lifetime of stratospheric aerosol optical depth (sAOD) (Kloss et al., 2021).

Muser et al. (2020) examined the impacts of aerosol-radiation interactions and aerosol dynamics on volcanic aerosol dispersion. They showed that during the first days after the Raikoke eruption, the absorption of solar radiation caused by the presence of ash had a significant impact on the aerosol dispersion, producing a self-lofting effect on the plume. Over the course of 4 days after the eruption, the maximum cloud top height rose more than 6km (Muser et al., 2020). Within a few weeks the

https://doi.org/10.5194/egusphere-2022-1060
Preprint. Discussion started: 26 October 2022

volcanic plume dispersed across the Northern Hemisphere (NH) and was continually observed months after the eruption. The radiative self-lofting could explain some of the differences between observations and model simulations which did not account for ash in previous studies (Haywood et al., 2010; Kloss et al., 2021) since the self-lofting effect would result in a greater fraction of the plume in the stratosphere and subsequently result in a longer residence time.

In Sect. 2 we introduce the observational data sets used and the differences in retrieval techniques. Furthermore, we provide a description of UKESM1, and the simulation set up in Sect. 3. In Sect. 4 we present the results and discussion before conclusions are drawn in Sect. 5.

2. Observational data and quality assurance

2.1 CALIOP

The Cloud-Aerosol Lidar and Infrared Pathfinder Satellite Observation (CALIPSO) satellite (Winker et al., 2009) combines an active lidar instrument with passive infrared and visible imagers to analyse the vertical structure and properties of thin cloud and aerosols. The CALIOP instrument is a dual-wavelength (532nm and 1064nm) polarization-sensitive lidar which provides high-resolution vertical profiles of aerosols and clouds. The aerosol profile products are reported at a uniform spatial resolution of 5km horizontally. The vertical resolution of the data varies as a function of altitude, with 60m vertical resolution in the troposphere and 180m vertical resolution in the stratosphere.

This study uses quality-assured (QA) daily averaged vertical profiles of aerosol extinction (km^{-1}) at 532nm from the Version 4.20 CALIOP Level 2 data product. These were mapped to a 1° x 1° latitude/longitude spatial grid whilst maintaining the original vertical profile. Quality control procedures were applied to the data in a similar fashion to those implemented in Campbell et al. (2012) which includes quality assurance on the stability of the retrievals and accounts for missing data when retrieval stability fails.

Active lidar retrievals, such as those obtained by CALIOP, are susceptible to solar background contamination which results in poorer performance in day-time conditions resulting in different minimum detection thresholds. It is estimated that the night-time threshold is 0.012 km^{-1} and the day-time thresholds is 0.067 km^{-1} (Toth et. al., 2018). The day-time detection threshold results in a column integrated underestimate of the AOD, and it has been found that it is unable to detect around 50% of aerosol profiles when the AOD is less than 0.1 (Toth et. al., 2018). For this reason, this study only uses the night-time retrievals to create the daily average extinction values to avoid an underestimated daily average. However, utilising only the night-time profiles leads to large areas of missing data, specifically at high latitudes during the Northern Hemisphere summer where areas experience 24 hours of sunlight. At most northern latitudes (60°N – 90°N) the CALIOP night-time profiles miss the initial peak in aerosol between 30 and 100 days after the eruption. Whilst the maximum night-time sAOD is approximately 65%

https://doi.org/10.5194/egusphere-2022-1060
Preprint. Discussion started: 26 October 2022

greater than the peak daytime sAOD, evaluating only the night-time profiles could influence the timing of the sAOD peak. This is discussed further in Sect. 4.

2.2 OMPS

The Suomi National Polar-orbiting Partnership (NPP) is a weather satellite which was launched in 2011 with five imaging systems, including the Ozone Mapping and Profiler Suite (OMPS), a series of instruments comprised of back-scattered ultraviolet radiation sensors. These sensors measure and monitor atmospheric trace gases, aerosols, surface reflectance and cloud-top pressure. There is global spatial coverage providing a good opportunity to evaluate the plume at high latitudes. Retrieved profiles have a vertical resolution of approximately 1.8km, with profiles being measured from the ground to about 80km (Taha et. al., 2021).

2.2.1: OMPS-NM: The OMPS Nadir Mapper (NM) measures backscattered UV radiance spectra between 300-380nm and whilst it is primarily designed to measure global total ozone, the SO_2 vertical column amount can be derived from the hyperspectral measurements of the OMPS-NM instrument. This study utilises the SO_2 Level 2 orbital products to assess the distribution of SO_2 after the eruption. A QA scheme is applied to daily profiles of total column SO_2 data, retrieved with a prescribed lower stratospheric profile centred at 16km above the surface. The screening includes discarding pixels when the solar zenith angle is greater than approximately 88° or viewing zenith angle is greater than approximately 70° (Yang, 2017).

2.2.2: OMPS-LP: In addition to the CALIOP aerosol extinction data, we utilise retrievals of the vertical aerosol extinction coefficient (km^{-1}) from the OMPS Limb Profiler (LP). The OMPS-LP is a passive sensor which looks back along the orbit track at the Earth's limb and records atmospheric spectra which are used to retrieve aerosol extinction coefficient profiles from the lower stratosphere (10 – 15km) to the upper stratosphere (55km). Aerosol extinction measurements are provided at wavelengths ranging between 510 – 997nm at 1km altitude intervals between the surface and 80km. This study utilises the V2.0 data measured at 869nm, which have been found to be the best OMPS-retrieved wavelength relative to SAGE III (Taha et al., 2021). Relative to V1.5 data, an improved cloud screening criterion is used in V2.0, which does not remove fresh volcanic plumes and allows us to use the filtered Retrieved Extinction Coefficient data product which removes the influence of polar stratospheric clouds (Taha et al., 2021). As with the CALIOP data, quality control procedures are applied to the OMPS-LP data. These include removing values where the cumulative residual error exceeds a threshold value, when the single scattering viewing angle exceeds 145° and where the derived aerosol scattering index is less than 0.01 (Johnson et al., 2020).

Due to the viewing geometry and sensitivity of the instrument, OMPS-LP can detect aerosol extinction coefficient values down to a minimum value of 1×10^{-5} km^{-1} (Johnson et al., 2020), which is far more sensitive than CALIOP (Section 2.1.1). However, OMPS-LP experiences loss of sensitivity of short wavelength radiances to aerosols, caused by Rayleigh scattering and aerosol attenuation of the limb scattered radiation, which is most pronounced below ~17km and in the southern hemisphere (Johnson

https://doi.org/10.5194/egusphere-2022-1060
Preprint. Discussion started: 26 October 2022

et al., 2020). The retrieval issues described here have a significant impact on our study since it was estimated that the initial plume reached altitudes of between 11 and 20km (Vaughan et al., 2021; Osborne et al., 2021). However, once the self-lofting of the plume occurs and it is dispersed over the northern hemisphere it is expected that the increased sAOD becomes more readily detectable by OMPS-LP (Hirsch and Koren, 2021), while it becomes less detectable or undetectable by CALIOP due to CALIOP's significantly higher minimum detection threshold. This is examined in more detail in Sect. 4.

2.3 AERONET

AERONET provides whole atmosphere AOD observations at a series of sites distributed across the globe providing a good global coverage of ground-based remote sensing data. One of these sites, the Mauna Loa Observatory (MLO), located at 3397m above sea level in Hawaii, provides an excellent opportunity to monitor stratospheric events. The measurement site is generally removed from the influence of pollution sources and is located at an altitude higher than most tropospheric aerosols. This provides an opportunity to retrieve ground-based observations of the stratosphere using sun-photometry with minimal tropospheric influences. MLO has been monitoring the stratospheric aerosol layer with lidars since 1975 (Barnes and Hofmann, 1997) providing a long-term historical record and previous studies have demonstrated that aerosol from the Raikoke plume was readily detectable (Chouza et al., 2020). Rather than lidars, this study uses daily Level 2 AOD AERONET retrievals measured at 500nm which are automatically cloud-cleared and quality assured.

3. Model simulations

3.1 UKESM1

UKESM1 is the latest UK Earth system model, described by Sellar et al. (2019). UKESM1 consists of the HadGEM3 coupled physical climate model with additional interactive components including modelling key biogeochemical processes (Yool et al., 2013), tropospheric and stratospheric chemistry (Archibald et al., 2020), aerosols (Mann et al., 2010) and sea-ice (Ridley et al., 2018). The atmosphere has a horizontal resolution of 1.25° latitude by 1.875° longitude with 85 vertical levels and a model top at around 85km (Storkey et al., 2018). Atmospheric composition in UKESM1 is simulated by the UK Chemistry and Aerosols (UKCA) sub-model. The StratTrop chemical mechanism used in UKESM1 is described by Archibald et al., (2019). This merged stratospheric and tropospheric scheme simulates interactive chemistry from the surface to the top of the model, including oxidation reactions responsible for sulfate aerosol production (Sellar et al., 2019).

3.2 Simulations

Simulations of the Raikoke and Ulawun eruptions were performed by nudging horizontal winds towards ERA5 reanalysis data to produce relevant meteorological conditions for the respective period using the atmosphere-only configuration of UKESM1. Nudged simulations were performed with no volcanic emissions as a control (CNTL), SO_2 emissions only (SO2only) and with SO_2 and ash emissions (SO2+ash). The Raikoke eruption was initiated for the 24-hour period starting at 00:00 UTC on 21st

https://doi.org/10.5194/egusphere-2022-1060
Preprint. Discussion started: 26 October 2022

June 2019. Emissions were injected into a single column within the model framework, but with vertical weights based on observations. In the vertical, there were two injection altitudes, a lower "tropospheric" injection at 10km and an upper "stratospheric" injection at 13-15km. A total of 1.5 Tg SO_2 (Kloss et al., 2021) was injected and, for the SO2+ash scenario, 1.1 Tg of ash (Muser et al., 2020) was also injected. Injection altitudes and masses of SO_2 and ash are consistent with observations and those found in the literature (Muser et al., 2020; Kloss et al., 2021; De Leeuw et al., 2021). The emission profile was weighted so that 80% was emitted into the stratosphere and the remaining 20% into the troposphere, based on observations of the SO_2 vertical profile (De Leeuw et al., 2021; Osborne et al., 2022).

Emissions of ash are implemented by adapting the Woodward (2011) bin scheme for mineral dust as a suitable proxy. The justification for doing this stems from the fact that the refractive indices and size distributions are similar (e.g. Millington et al., 2012; Johnson et al., 2012; Osborne et al., 2022), although it is recognised that substantial inter-eruption and inter-eruption-phase variability in volcanic ash refractive indices occurs (e.g. Millington et al., 2012; Turnbull et al., 2012).Transport and deposition of dust is as described in detail in Woodward (2001) with improvements to the emission scheme and refractive index data described in Woodward (2022). Volcanic ash size distributions were based on observations of the Eyjafjallajökull eruption presented in Johnson et al. (2012) fitted by lognormal distributions (Table 5 of Johnson et al., 2012). In the current configuration dust is externally mixed with other aerosols.

For both SO2only and SO2+ash simulations, the Ulawun eruptions are simulated by UKESM1 with an SO_2 only injection (no ash emissions) and are initiated on 26th June and 3rd August 2019. Injection altitudes for Ulawun were 13-17km (26th June) and 14-17km (3rd August) using 0.14 Tg and 0.30 Tg SO_2 respectively (Kloss et al., 2021).

3.3 Mie scattering calculations

To facilitate the intercomparison of the observations and the model simulations all datasets were scaled to 532nm. Mie scattering calculations were performed using the Mie code within SOCRATES (Suite Of Community RAdiative Transfer codes based on Edwards and Slingo; Edwards and Slingo, 1996) to generate the single scattering properties of volcanic aerosol at a range of specified wavelengths. The size distribution of the volcanic aerosol used here was based upon the bimodal lognormal size distribution for a moderate loading volcanic eruption (SPARC, 2006). Specific extinction coefficients were calculated to allow all observational and model data to be scaled to one consistent wavelength; 532nm.

4. Results

In analysing the results, we attempt to follow a logical timeline from the injection of the SO_2 and ash through to the gas phase oxidation of the SO_2 to sulfate aerosol and the ultimate deposition of the aerosol until the stratospheric perturbation is no longer

https://doi.org/10.5194/egusphere-2022-1060
Preprint. Discussion started: 26 October 2022

detectable. Different aspects are investigated including the geographic distribution and temporal evolution of the SO_2 and sulfate aerosol and the latitudinal distribution and vertical profile of the sulfate aerosol.

4.1 Observed and modelled SO_2 including and excluding volcanic ash

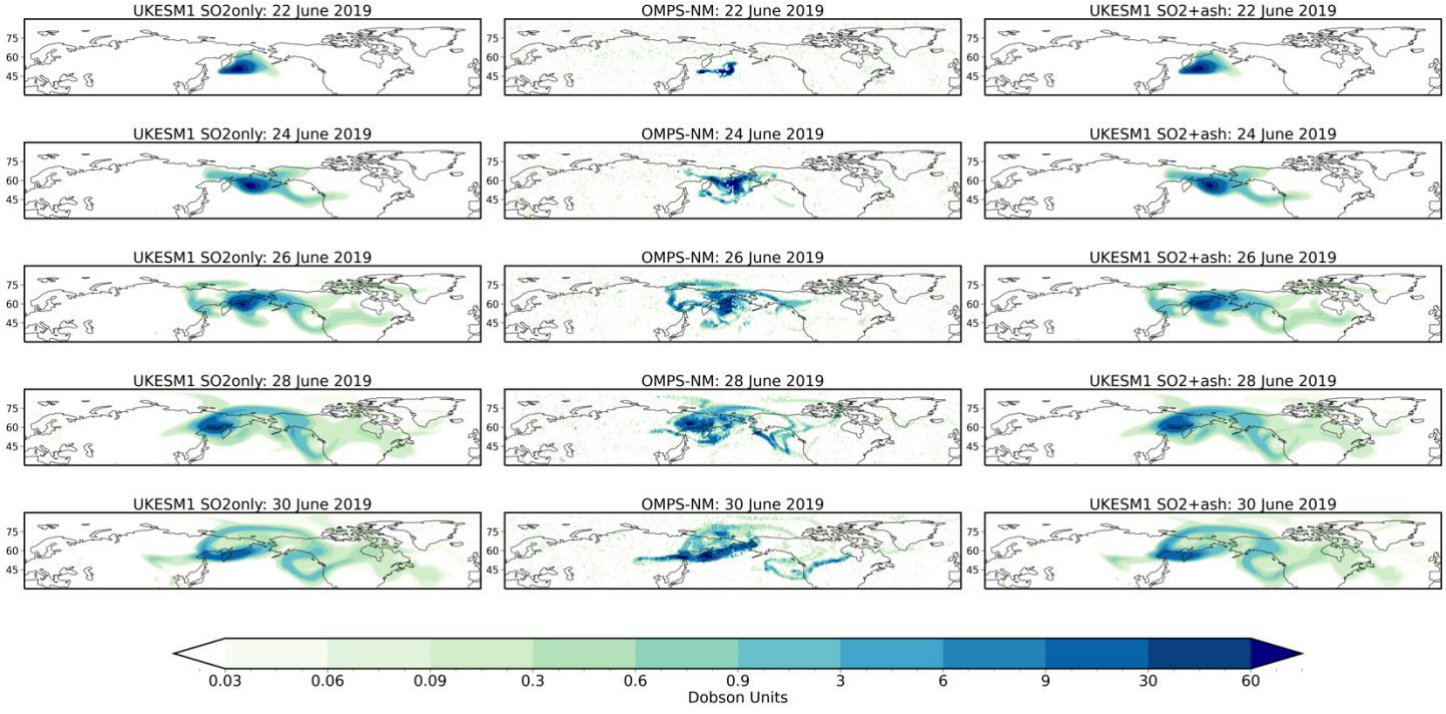

Figure 1: Geographic evolution of column integrated SO_2 plume in Dobson Units (DU) derived from OMPS-NM lower stratospheric profile (centre) UKESM1 SO2only (left) and SO2+ash (right) for the period 22–30th June 2019. We remove the long-term background SO_2 burden derived from OMPS-NM for the years 2013–2018 from those for 2019 to provide a stratospheric perturbation for the observations. Similarly, we remove the impacts of background stratospheric aerosol from the model simulations by subtracting the stratospheric sulfate burdens from the CNTL simulation from those for SO2only and SO2+ash.

Figure 1 shows the evolution of the SO_2 cloud from 22nd June through to the 30th June 2019. The middle column shows the OMPS-NM observations, with the UKESM1 SO2only and SO2+ash simulations on the left and the right respectively. We see that the position and timing of the plume is relatively well modelled throughout this period in both simulations. There is little difference in the spatial pattern of the SO_2 plume in both simulations, making it difficult to determine based upon SO_2 alone which simulation best represents the observations. Qualitatively, the spatial pattern of the plume is better represented in the model simulations from 26th June onwards, with both the easterly and westerly parts of the plume well modelled. The largest

https://doi.org/10.5194/egusphere-2022-1060
Preprint. Discussion started: 26 October 2022

240 difference between the observations and the model simulations is seen on 22nd June where the model is initially much more diffuse. This is due to the eruption taking place at 18:00 UTC 21st June and was inherently explosive and sporadic in nature compared to the smooth injection rates that are assumed in the model. This could explain why the modelled plume does not represent the observations as well during the first two days after the eruption. However, since the model does a reasonable job at representing the shape and distribution of the plume after a few days, and our objectives are to assess the general model
245 performance over a period of many months, we retain our simplified emission time and altitudes. Higher resolution modelling assessments using the Met Office Numerical Atmospheric-dispersion Modelling Environment (NAME), that are more appropriate for operational monitoring of volcanic plumes for the first few weeks after the eruption for the purposes of aviation safety are available in de Leuuw et al., (2021) and Osborne et al., (2022).

250 In the first few days after the eruption the SO_2 plume becomes trapped within a cyclonic circulation across Eastern Russia and Alaska (e.g. Osborne et al., 2022). We can observe this feature in both the observations and the model simulations. However, as observed in other similar studies of other volcanic eruptions (e.g., Haywood et al., 2010) the model SO_2 plume becomes more diffuse than observations over time. We can see that as the plume evolves, despite the model capturing the general position, the model overestimates the tail crossing North America and underestimates the magnitude of the plume over Russia.
255 This can also be due to the instrumental detection limits, where the plume has become so diffuse it becomes undetectable.

To provide a more quantitative analysis of the geographic evolution we employ a dichotomous forecast style analysis. A contingency table is a simple way to identify the frequency of "yes, an event will happen" and "no, the event will not happen" forecasts and occurrences. For this analysis we treat the model simulation as the forecast and the observations as the occurrence
260 for each grid box on each day. There are four combinations of simulations and observations, "*hits"* – the model simulates the observations correctly, "*model > observations"* – the model overestimates the observations, "*observations > model"* – the model underestimates the observations and "*correct negative"* – both the observations and the model are below a given threshold, 0.3 Dobson Units (DU). In developing the contingency table we consider estimates of error such as timing errors in synoptic meteorological features that frequently occur in weather forecasting and the fact that the model and observations are
265 not perfectly collocated in time. We therefore assume that the observations are uncertain by a factor of two and use these as the upper and lower bounds. However, we recognise that much more detailed and comprehensive approaches to forecast verification have been developed (e.g. Casati et al., 2008).

Figure 2 presents this analysis for the first 10 days after the eruption. Both simulations show a similar distribution, so we focus
270 on SO2only here. It is clear that "*model > observations*" dominates, with a large tail over North America, as seen in Figure 1. However there are some regions where the model is underestimating the observations which may not have been identified by eye in Figure 1. Over the 20 days after the eruption, approximately the time for the oxidation of SO_2 to sulfate aerosol, both model simulations overestimate the observed plume 52% of the time. We also note that between 15 – 17% of the plume is

https://doi.org/10.5194/egusphere-2022-1060
Preprint. Discussion started: 26 October 2022

correctly modelled within the bounds of the observations for both simulations, with SO2+ash underestimating the observations 3% more than SO2only.

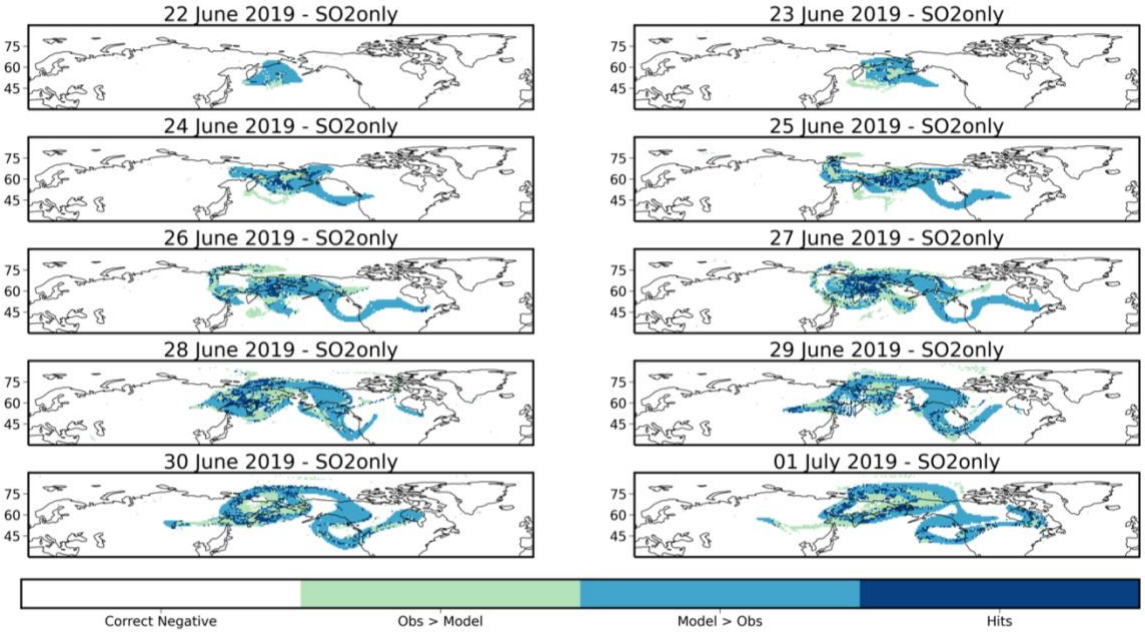

Figure 2: Contingency analysis of SO_2 plume between OMPS-NM lower stratospheric profile and UKESM1 SO2only for the period 22nd June–1st July 2019. "Correct Negative" occurs at the point where both the model and observation are below 0.3 DU. "Hits" occur at the point where the modelled column SO_2 burden is within a factor of two of the observations at that point to allow for timing errors. "Obs > Model" and "Model > Obs" occur when the modelled column SO_2 burden is above or below the factor of two limit.

In Figure 1 we can see that the SO_2 plume travels longitudinally and moves towards more northern latitudes, as we would expect from the stratospheric Brewer-Dobson circulation (e.g. Haynes, 2005), and as evidenced from the previous eruption of Sarychev Peak (Haywood et al., 2009; Jégou et al., 2013). Due to this poleward transport, it is unlikely that the Raikoke SO_2 plume would travel south of 30°N, particularly in the first few months after the eruption. Hence, to avoid any influence from the Ulawun eruption we take the area weighted average from 30 – 90°N (discussed further in Sect. 4.3) to determine the temporal evolution of SO_2 and calculate an *e*-folding time. Figure 3 shows the daily column burden of observed and modelled SO_2 after the eruption. The observations show a peak column burden of 0.76 DU and have an *e*-folding time of 20 days. Model simulations had similar *e*-folding times of 19 and 21 days for SO2only and SO2+ash respectively. This suggests that the oxidation processes are well represented in the UKESM1 model and are very similar to those determined for the Sarychev Peak eruption for the fore-running HadGEM-2 climate model (Haywood et al., 2010). However, in both SO2only and SO2+ash

https://doi.org/10.5194/egusphere-2022-1060
Preprint. Discussion started: 26 October 2022

model simulations the peak SO_2 column burden is only 0.44 DU, considerably less than that observed by OMPS-NM. The notable difference between the observations and the model is unexpected given that the magnitude of SO_2 injected was based on observations (Muser et al., 2020; Kloss et al., 2021; De Leeuw et al., 2021). However, if the amount of SO_2 injected into the model simulations were to be increased it would lead to a significant overestimate of sulfate aerosol and sAOD (see later sections). For this reason we do not change the amount of SO_2 injected.

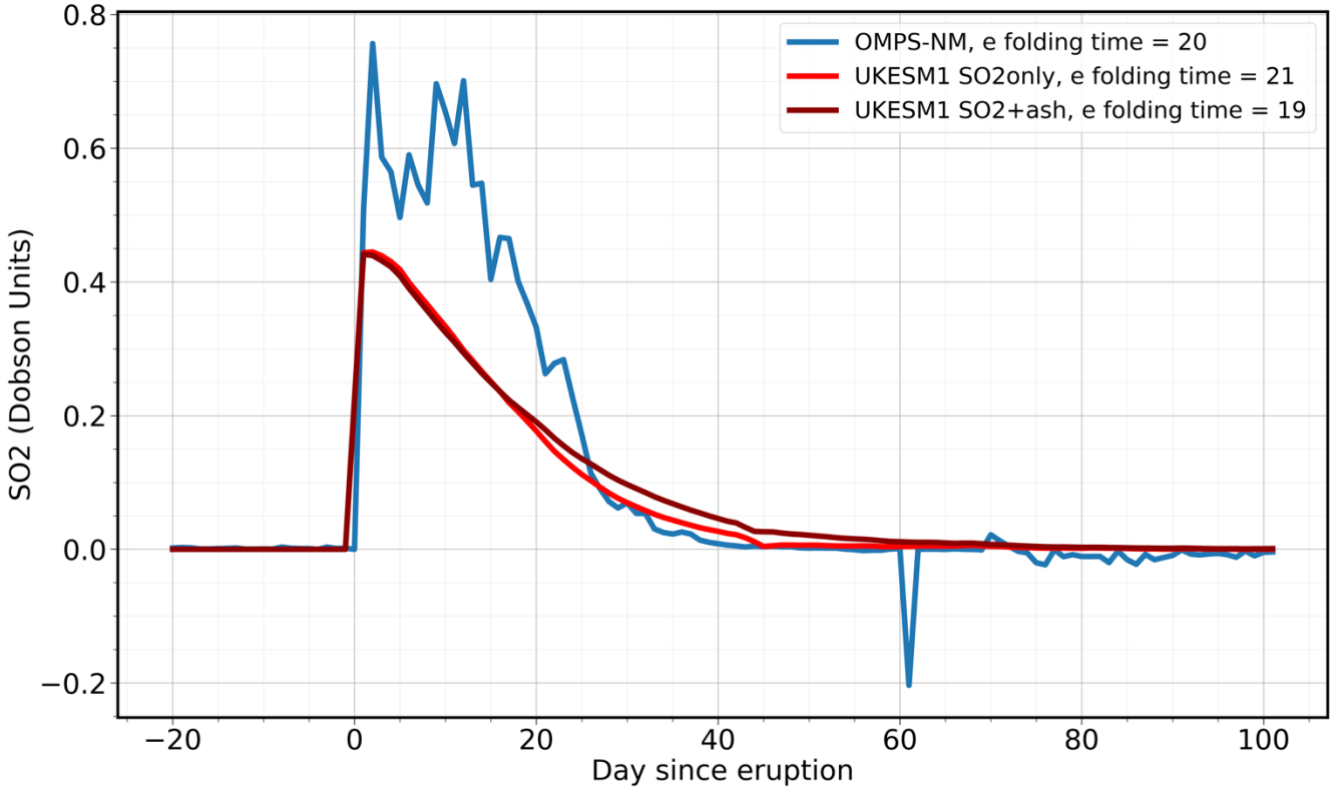

Figure 3: Daily perturbation of SO_2 in Dobson Units (DU) derived from OMPS-NM lower stratospheric profile (blue), UKESM1 SO2only (red) SO2+ash (dark red). Data averaged across latitudes 30–90° N, weighted by the cosine of the corresponding latitude to ensure data is area weighted. We remove the long-term background SO_2 burden derived from OMPS-NM for the years 2013–2018 from those for 2019 to provide a stratospheric perturbation for the observations. Similarly, we remove the impacts of background stratospheric aerosol from the model simulations by subtracting the stratospheric sulfate burdens from the CNTL simulation from those for SO2only and SO2+ash.

https://doi.org/10.5194/egusphere-2022-1060
Preprint. Discussion started: 26 October 2022

4.2 Distribution of sulfate aerosol

To investigate the distribution and evolution of the sulfate plume we utilise the CALIOP and OMPS-LP retrieved aerosol extinction integrated above the tropopause to find the perturbed sAOD. We firstly investigate the temporal evolution of the zonal mean sAOD by performing similar analysis to previous studies (e.g., Kravitz et al., 2010; Haywood et al., 2010; Kloss et al., 2021). We compare the evolution of the OMPS-LP and CALIOP retrievals against the UKESM1 SO2only and SO2+ash scenarios, shown in Figure 4. Due to the differences in satellite retrievals discussed in Section 2, there are seasonal gaps in the data from as far south as ~55°N in CALIOP night-time retrievals, due to polar summer and ~65°N in OMPS-LP due to the lack of daylight hours in NH winter. Additionally, the observations have different minimum retrieval limits (0.012 km^{-1} for CALIOP, 1 x 10^{-5} km^{-1} for OMPS-LP) so to ensure better comparisons we have applied both requirements to both model simulations and scaled all data to a wavelength of 532nm.

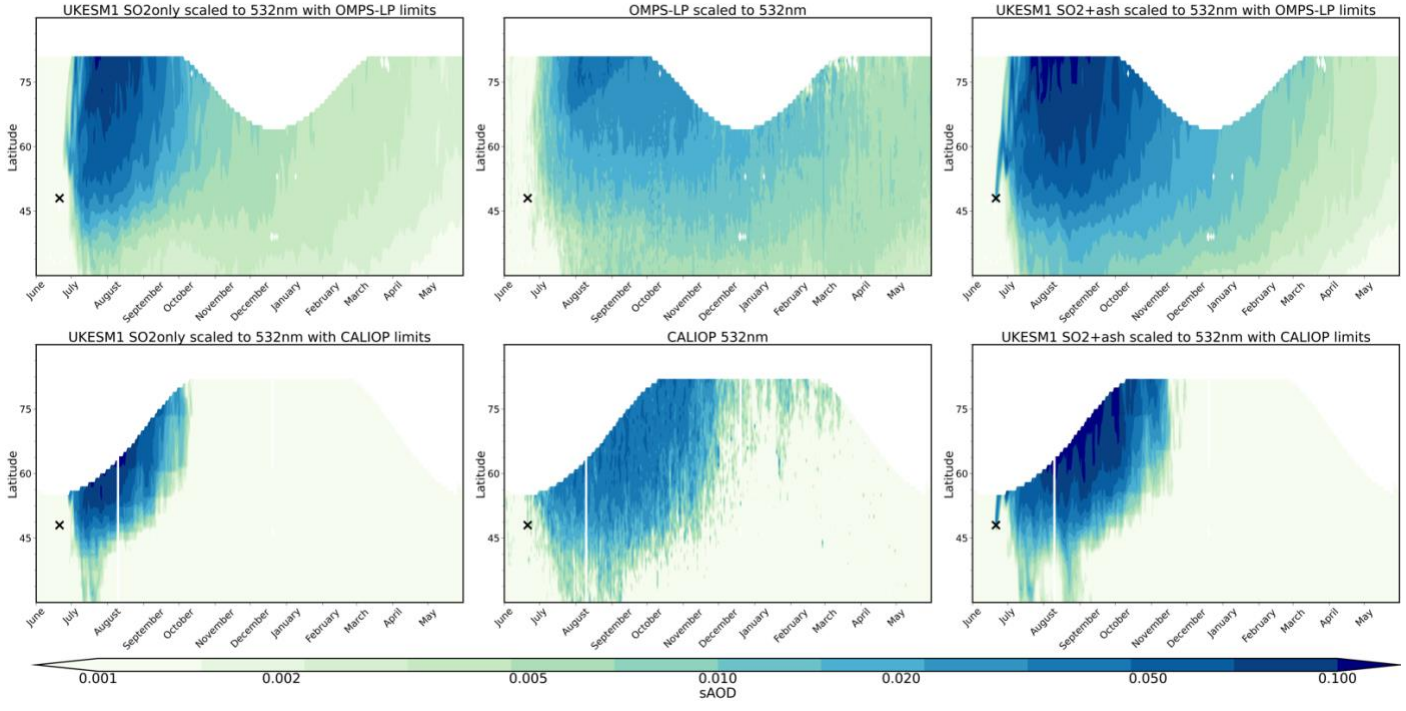

Figure 4: Latitude-time distribution of the longitudinally averaged sAOD from 30–90° N. (a) UKESM1 SO2only masked for OMPS-LP observations, scaled from 550nm to 532nm (b) UKESM1 SO2only masked for CALIOP observations, sAOD calculated with values of aerosol extinction < 0.012 km-1, the CALIOP minimum detection limit, scaled to 532nm (c) OMPS-LP observations scaled from 869nm to 532nm (d) CALIOP observations at 532nm (e) UKESM1 SO2+ash masked for OMPS-LP observations, scaled from 550nm to 532nm (f) UKESM1 SO2+ash masked for CALIOP observations, sAOD calculated with values of aerosol extinction < 0.012 km^{-1}, the CALIOP minimum detection limit, scaled to 532nm. The location of Raikoke is marked with a black cross.

https://doi.org/10.5194/egusphere-2022-1060
Preprint. Discussion started: 26 October 2022

Fig. 4c shows the evolution of zonal mean sAOD derived from OMPS-LP from June 2019 to May 2020. The zonal peak sAOD occurs ~1.5 months after the eruption, which is similar to the findings in Gorkavyi et al., 2021. The impact on the sAOD in OMPS-LP is still present one year later, with values of sAOD not yet returned to their pre-eruption values. This contrasts with Fig. 4d, the same quantity derived from CALIOP, where the perturbation of sAOD is significantly reduced by December 2019 and by March/April 2020 zonal sAOD values are similar to those found pre-eruption. We can confidently attribute this difference in aerosol lifetime to the high aerosol extinction minimum detection threshold for aerosol extinction associated with the CALIOP dataset. Figs. 4b and 4f display the UKESM1 SO2only and SO2+ash zonal mean sAOD with the CALIOP minimum retrieval limits applied where a similar distribution to that seen in the observations is modelled, indicating that the shorter aerosol lifetime observed in the CALIOP retrievals compared to OMPS-LP is due to high detection limits. As the plume disperses over time the plume becomes more diffuse and becomes undetectable by CALIOP, leading to under-detection and hence the integrated sAOD reduces much more rapidly than we see in the OMPS-LP data.

In both sets of observations (Figure 4c and 4d) we can see that the enhanced stratospheric aerosol layer has been transported poleward by the Brewer-Dobson circulation with the highest sAODs found north of the eruption. The model simulations represent this transport relatively well with similar distributions to both OMPS-LP and CALIOP observations. However, in all cases the peak magnitude is over estimated, especially in the SO2+ash case. Whilst the peak sAOD in the SO2only simulation (Fig. 4a and 4b) is less of an overestimate of the observations compared to SO2+ash, it does not reproduce the evolution of the plume as well as the SO2+ash simulation (Fig. 4e and 4f) in either case. Despite the SO2+ash simulation (Fig. 4f) representing the CALIOP retrievals well it is not representative of how the plume evolves over time after becoming too diffuse for CALIOP detection limits. However, as OMPS-LP has a much lower minimum detection threshold as a dedicated stratospheric limb-profiler the decay rate of sAOD is much slower. We see a similar decay rate in the SO2+ash simulation (Fig. 4e) with comparable magnitudes to the OMPS-LP observations from December onwards. From Fig. 4 we can begin to infer that the SO2+ash simulation represents the evolution of zonal sAOD better than the SO2only case, but this inference is far from conclusive. Further comparisons to the model are made in Sect. 4.4.

4.3 Temporal evolution of sulfate aerosol

The CALIOP and OMPS-LP derived perturbations of sAOD from the long-term mean are presented in Figure 5. As seen in Fig. 4 the two satellite observations have different temporal evolutions. Comparing the early stages of the plume evolution it is clear that OMPS-LP does not detect the same high peak in sAOD as CALIOP. The CALIOP dataset shows a clear peak 60 days after the eruption with an sAOD of approximately 0.026 whereas, OMPS-LP reaches a peak sAOD of approximately 0.015 over 3 months after the eruption. Studies have suggested that limb-instruments such as OMPS-LP can fail to detect aerosol near the tropopause (e.g., Fromm et al., 2014). However, since CALIOP is a nadir viewing lidar the altitude of the plume does not significantly affect the retrieval. This could result in the difference we see in the initial sAOD peaks since the

https://doi.org/10.5194/egusphere-2022-1060
Preprint. Discussion started: 26 October 2022

plume was detected at altitudes as low as 11km (Hedelt et al., 2019; Vaughan et al., 2020). The vertical profile of the plume is explored further in Section 4.6. We also see a big difference in the decay rate of sAOD. The CALIOP observations have an *e*-folding time of 84 days, in comparison to OMPS-LP which has an *e*-folding time of 220 days. As previously discussed, the difference in decay rate between CALIOP and OMPS-LP is likely due to the different minimum detection thresholds for both satellites. Once the plume begins to dilute and become more diffuse the higher CALIOP detection threshold (0.012 km^{-1}) results in under-detection in comparison to OMPS-LP which has a much lower threshold (1 x 10^{-5} km^{-1}) and is thus able to detect more of the diffuse plume.

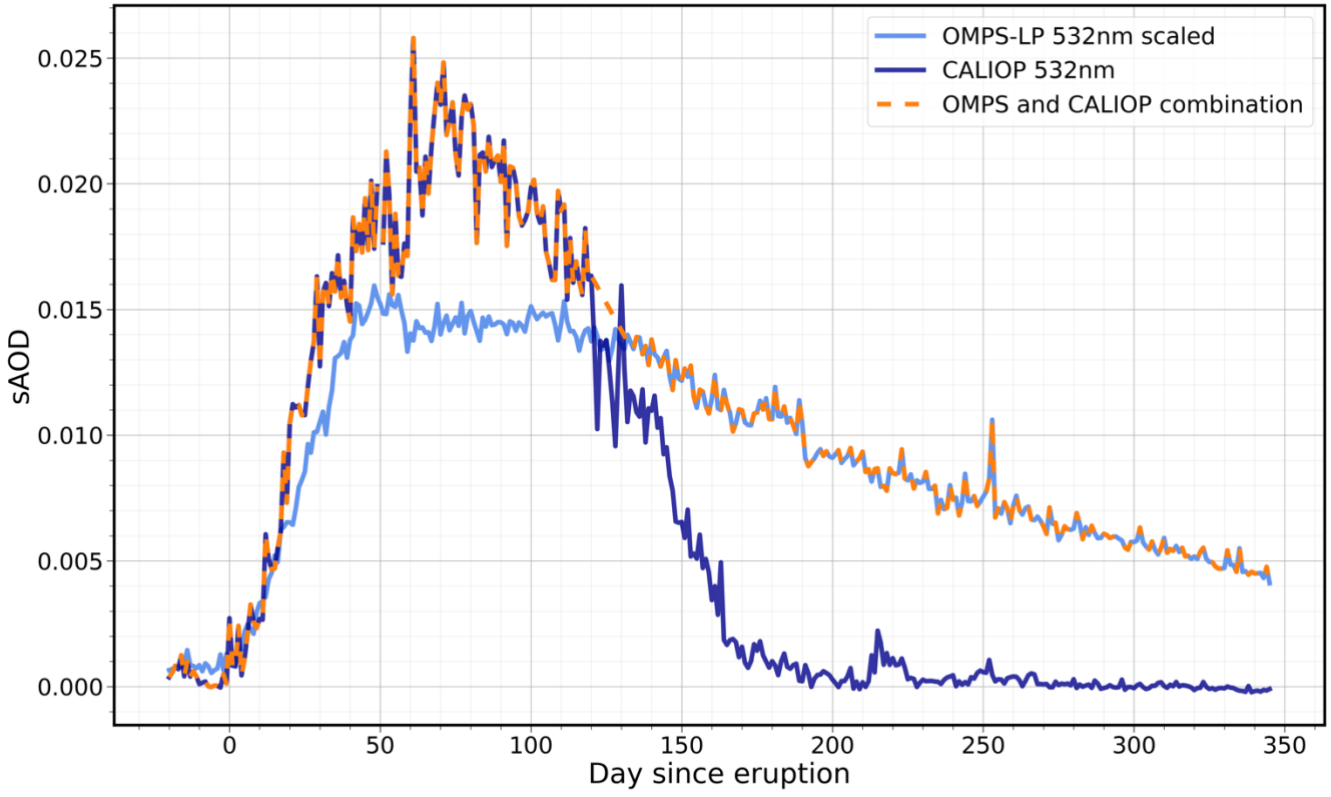

Figure 5: Daily perturbation in the sAOD averaged over 30–90° N as observed by OMPS-LP scaled from 510nm to 532nm (light blue) and CALIOP at 532nm (dark blue). The orange dashed line represents the combined OMPS-LP and CALIOP dataset at 532nm. We remove the long-term background sAOD derived from OMPS-LP and CALIOP for the years 2013–2018 from those for 2019 to provide a stratospheric perturbation for the observations.

We have created a combined dataset which includes aerosol extinction data from both CALIOP and OMPS-LP, seen in Fig. 5. The combined dataset utilises the area averaged (30 - 90°N) CALIOP sAOD data for the first 4 months after the eruption before it is linearly interpolated over the region in which the two datasets cross over and then employs OMPS-LP data for the

https://doi.org/10.5194/egusphere-2022-1060
Preprint. Discussion started: 26 October 2022

remaining months. This new dataset has an *e*-folding time of 145 days, and we believe that it is more physically reasonable than using a single observational dataset due to the data constraints outlined above. To confirm qualitatively that using the OMPS-LP data is more appropriate than CALIOP in the later months after the eruption we use in-situ ground-based data to provide an alternative comparison to these satellite datasets. We utilize the AERONET Level 2 AOD retrievals measured at 550nm and scale them to 532nm for comparison with the satellite observations. To calculate the satellite retrievals at MLO an area average is taken across multiple grid boxes encompassing the MLO. Note that AERONET retrievals of sAOD are not a point measurement as they are a function of the solar zenith angle. For solar zenith angles of 60-80 degrees and assuming that any aerosol is located in the lowest 20km above the observatory, aerosol within a 35-115km radius is included in the observations. The same area is used to calculate the average monthly SO2only and SO2+ash perturbations.

	AERONET	OMPS-LP	CALIOP	UKESM1 SO2only	UKESM1 SO2+ash
August	5.89×10^{-3}	**2.16×10^{-3}**	-0.01×10^{-3}	2.78×10^{-3}	4.27×10^{-3}
September	**12.12×10^{-3}**	**7.07×10^{-3}**	0.06×10^{-3}	3.03×10^{-3}	8.46×10^{-3}
October	**9.78×10^{-3}**	**6.41×10^{-3}**	0.08×10^{-3}	3.33×10^{-3}	7.12×10^{-3}
November	**4.70×10^{-3}**	**4.89×10^{-3}**	-0.01×10^{-3}	2.91×10^{-3}	5.40×10^{-3}
December	1.05×10^{-3}	**3.81×10^{-3}**	0	2.12×10^{-3}	3.96×10^{-3}
Average	6.71×10^{-3}	4.87×10^{-3}	0.01×10^{-3}	2.83×10^{-3}	5.84×10^{-3}

Table 1: Perturbation of AOD from the long-term mean retrieved from the Mauna Loa Observatory AERONET site scaled to 532nm. OMPS-LP, CALIOP, UKESM1 SO2only and SO2+ash sAOD perturbation calculated across an area encompassing the MLO (19–20° N, 152–156° W). Observations highlighted with bold text are statistically significantly greater than the long-term mean at 95% confidence level. Negative values of AOD are a result of calculating the perturbation from the long-term mean (2013–2018).

Average monthly perturbations from the long-term mean (or control simulation) for the Mauna Loa observatory, are presented in Table 1. The AERONET retrievals are statistically significant from the long-term mean from September to November and increase to a peak AOD of 12.12×10^{-3} in September, over 2 months after the eruption. The OMPS-LP retrievals and SO2+ash model show a similar pattern with peak AODs in September of 7.07×10^{-3} (OMPS-LP) and 8.46×10^{-3} (SO2+ash). The SO2only simulation follows a similar pattern of increased AOD between August and November, however the magnitude of AOD is much smaller than the AERONET and OMPS-LP observations. OMPS-LP retrievals are also significantly greater than the long-term mean from August through until December. CALIOP however does not appear to detect any statistically

https://doi.org/10.5194/egusphere-2022-1060
Preprint. Discussion started: 26 October 2022

significant perturbation to the sAOD, with values an order of 10^2 smaller than those observed by AERONET and OMPS-LP. This is most likely due to the minimum detection threshold and the plume becoming more diffuse at this latitude. We also calculate the average perturbed AOD for this region from August to December, presented in Table 1. The SO2+ash average AOD, 5.84 x 10^{-3}, agrees well with the AERONET and OMPS-LP observations, 6.71 x 10^{-3} and 4.87 x 10^{-3} respectively. However, the SO2only average AOD is much smaller suggesting that the SO2+ash simulation validates better against this specific set of observations.

MLO is located at 19.5°N, around 30° south of Raikoke. As we observed in Fig. 4 most of the aerosol plume travelled poleward via the Brewer-Dobson circulation, however there was some southern transport seen in both satellite observations in late July and August. We can observe this further in Figure 6, the monthly average sAOD observed by OMPS-LP and CALIOP.

Figure 6 shows the monthly geographic evolution of the sAOD in the Northern Hemisphere. MLO is highlighted on the first plot by a red cross. From this plot we can see that transport to lower latitudes does not occur until August, however the CALIOP retrievals are much more diffuse than those observed in OMPS-LP. We observe high values of sAOD at high latitudes with peaks across Greenland and Northern Canada. Despite the missing data in the CALIOP observations we can still see a reasonable spatial agreement in the sAOD during the first few months. In December an interesting feature is seen in the OMPS-LP data where a band of enhanced sAOD is observed between 0 – 15°N. This might be attributed to the second Ulawun (5.05°S, 151°E) eruption on 3rd August which, owing to the latitude and altitude of the eruption is likely to be confined by the so-called "tropical pipe" between approximately 15°S-15°N (e.g. Plumb, 1997), although some leakage to higher latitudes might be expected over time. From August onwards the stratospheric aerosol layer south of the equator has been shown to become enhanced. Kloss et al., (2021) estimate that the aerosol from the Ulawun eruption circled the Earth in the tropics within one month. During October and November the sAOD in the tropical stratosphere becomes increasingly enhanced, which is likely due to the influence of Ulawun. Due to the influence of Ulawun this study uses area averages from 30 – 90°N to ensure analysis focuses solely on the impact of the Raikoke eruption. Despite the potential influence of Ulawun on MLO observations, we can nevertheless conclude that combining CALIOP and OMPS-LP is the most appropriate representation of the plume evolution since OMPS-LP does not observe the initial peak while CALIOP detection limits lead to non-detection of aerosol once it has become diffuse hence apparently reducing the observed lifetime and e-folding time of the sulfate aerosol.

https://doi.org/10.5194/egusphere-2022-1060
Preprint. Discussion started: 26 October 2022

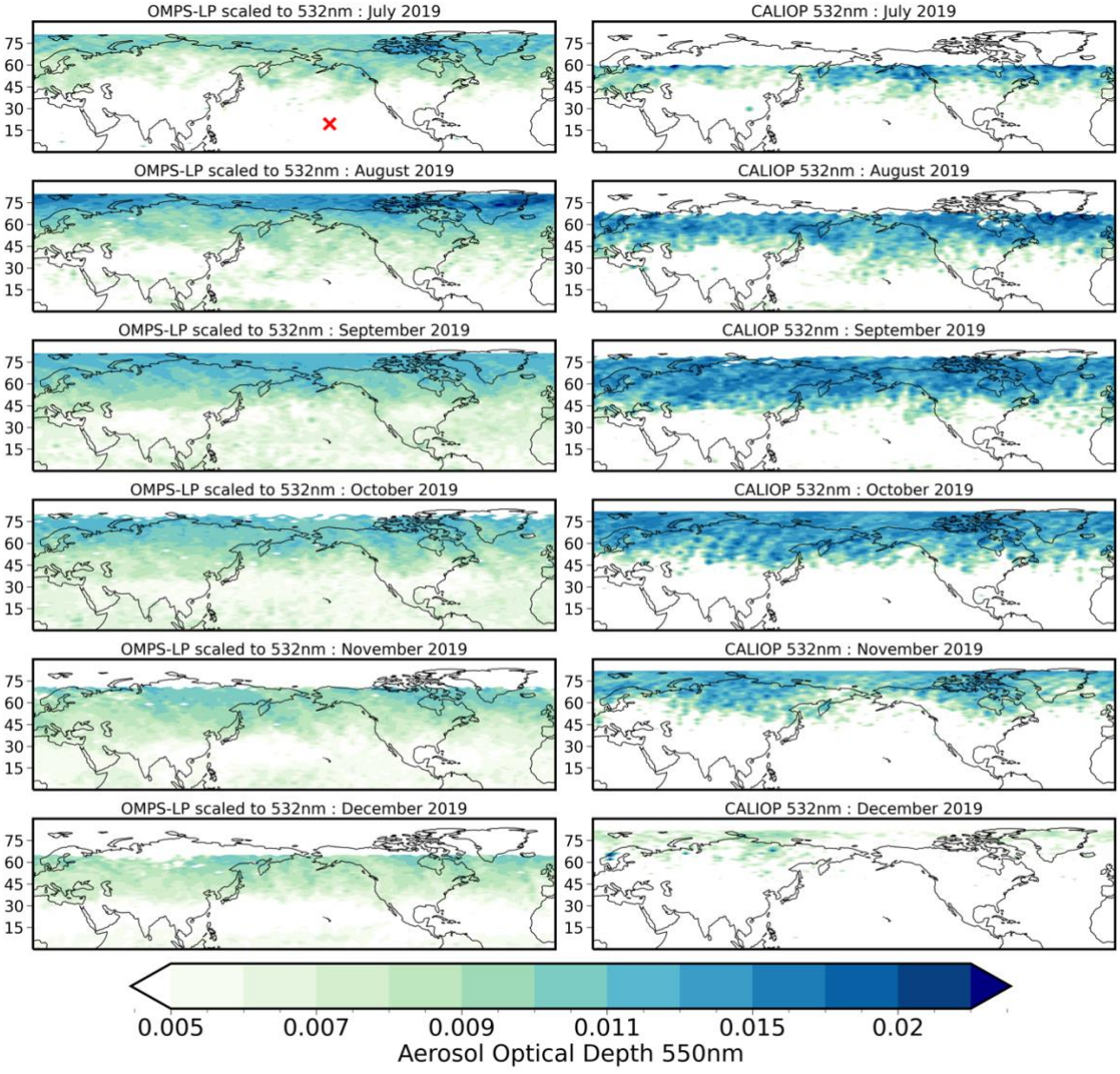

425 **Figure 6:** Monthly geographic evolution of the Northern Hemisphere sAOD from July 2019 to December 2019 derived from OMPS-LP Retrieved Aerosol Extinction (left) and CALIOP Aerosol Extinction Profile (right). We remove the long-term background sAOD derived from OMPS-LP and CALIOP for the years 2013–2018 from those for 2019 to provide a stratospheric perturbation for the observations.

https://doi.org/10.5194/egusphere-2022-1060
Preprint. Discussion started: 26 October 2022

4.4 Model comparison

To make consistent and accurate comparisons between the combined satellite dataset and the model simulations it is appropriate to implement the same method used in Fig. 4 and apply minimum detection and spatial limits to the model data. Since the combined dataset uses the CALIOP observations initially we implement the CALIOP minimum detection threshold in the SO2only and SO2+ash simulations for the first 4 months after the eruption. After this we apply the limits of the OMPS-LP data to the model for the remaining days. No linear interpolation was applied to the SO2only and SO2+ash simulations when observational limits are applied owing to the considerable difference in sAOD across the area of interpolation. Figure 7 compares the combined OMPS-LP and CALIOP dataset to the two model simulations both with (solid lines) and without (dashed lines) the respective observational limits applied.

Figure 7 begins to illustrate the extent to which the SO2only and SO2+ash simulations differ. The SO2only case, both with and without limits has a much faster decay rate in comparison to both the observations and SO2+ash scenario. As we observed in Fig. 4 the peak sAOD is overestimated in both model scenarios, both with and without observational limits applied. We also note that the timing of the peak is much earlier in SO2only compared to the observations. The combined observational dataset peaks at approximately 0.026 around 2 months after the eruption and has an *e*-folding time of 145 days. In the SO2only scenario without limits applied, the peak sAOD is 0.039 occurring almost 30 days after the eruption. Even with observational limits applied the peak sAOD is still much greater (0.033) and earlier than observations. Without the observational limits applied, SO2only has an *e*-folding time of 45 days, over 3 months faster than the observations. We observe a similarly fast decrease in sAOD when observational limits are applied to SO2only, whereby approximately 4 months after the eruption the sAOD drops to zero before an increase at approximately day 135 after the eruption. This is an artifact of combining CALIOP and OMPS-LP limits to the SO2only simulation to best compare against the combined observational dataset.

In contrast to the SO2only simulation, there is a large difference between the early stages of the SO2+ash model with and without limits. There is a difference in both the magnitude and the timing of the sAOD peak. When observational limits are applied SO2+ash has a faster *e*-folding time and smaller peak sAOD which we can attribute to the high CALIOP minimum detection threshold. The delay in the peak of sAOD when limits are applied can be attributed in part to the missing data at high latitudes during the polar summer, which can be observed in the model when only spatial limits are applied. This delay is not seen as greatly in the SO2only scenario; however it is more noticeable when spatial limits are applied without the CALIOP detection limits. We can see in both Fig. 4 and 6 the sulfate aerosol travels poleward due to the Brewer-Dobson circulation and the resulting sAOD would most likely be greatest within the first few months. However, due to the time of year there are no CALIOP night retrievals in this area which results in a delayed aerosol peak.

https://doi.org/10.5194/egusphere-2022-1060
Preprint. Discussion started: 26 October 2022

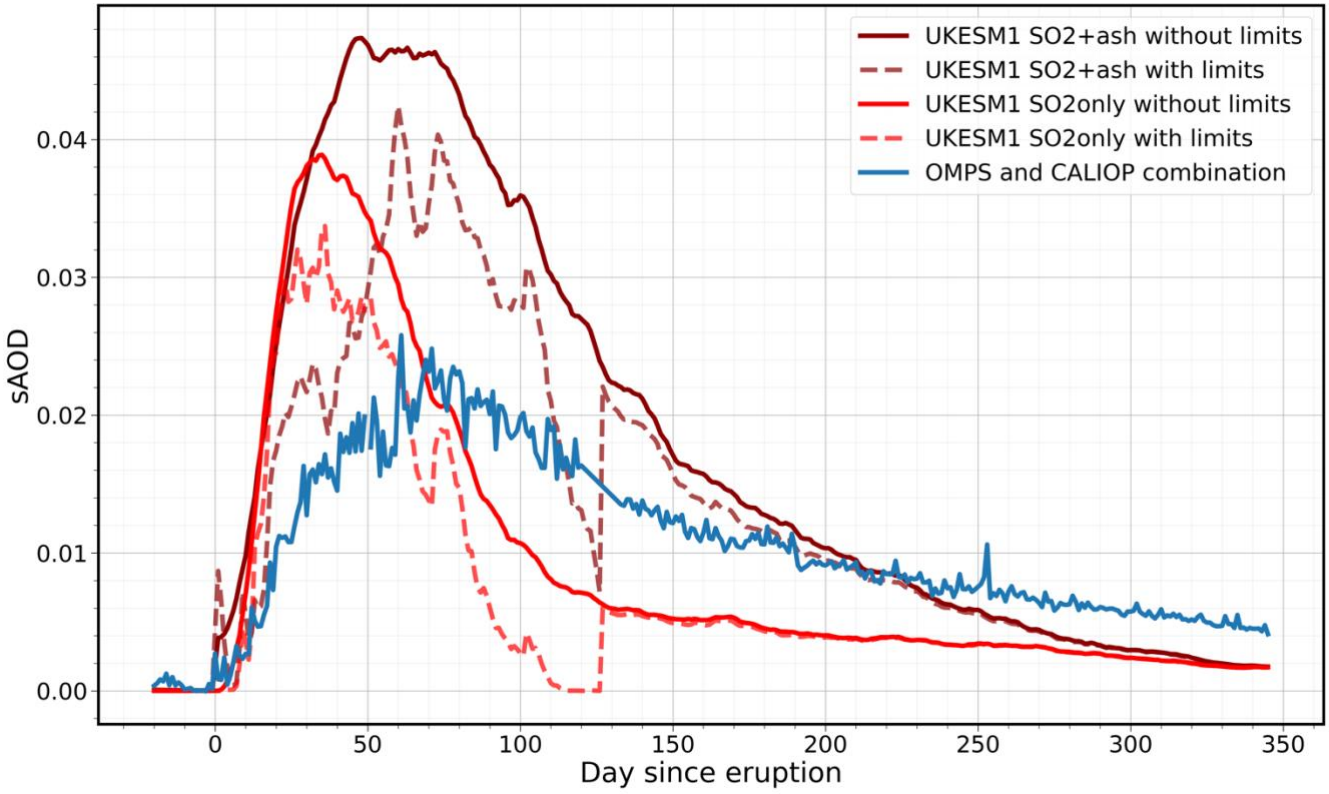

Figure 7: Daily perturbation of sAOD at 532nm averaged over 30–90° N. Daily OMPS-LP and CALIOP combined dataset sAOD (blue), UKESM1 SO2only with observational limits applied (red) and without limits applied (red dashed) and UKESM1 SO2+ash with observational limits applied (dark red) and without limits applied (dark red dashed). We remove the long-term background sAOD derived from OMPS-LP and CALIOP for the years 2013–2018 from those for 2019 to provide a stratospheric perturbation for the observations. Similarly, we remove the impacts of background stratospheric aerosol from the model simulations by subtracting the sAOD from the CNTL simulation from those for SO2only and SO2+ash.

The SO2+ash model with observational limits peaks at a similar time to the observations, however the magnitude of sAOD is almost double at 0.042. We then observe a decline in model sAOD owing to transfer from the stratosphere to the troposphere with an *e*-folding time of 90 days, almost 2 months faster than the observed data. The initial steep decline in SO2+ash is due to the CALIOP limits imposed upon the model. At approximately day 135 after the eruption there is a sharp increase in modelled sAOD. Similarly to SO2only, this is an artifact of combining SO2+ash with CALIOP limits and SO2+ash with OMPS-LP limit. The SO2+ash simulation with CALIOP limits applied has a much faster decay rate with an *e*-folding time of 44 days, whereas the SO2+ash simulation with OMPS-LP limits has a much longer *e*-folding time of 101 days. Whilst SO2+ash is not perfect at recreating the sAOD evolution, we can see that by applying the observational limits it starts to become apparent that SO2+ash provides a better comparison against observations than SO2only, although some considerable differences still

https://doi.org/10.5194/egusphere-2022-1060
Preprint. Discussion started: 26 October 2022

exist. In the following two sections we explore changes to the stratospheric aerosol Ångström Exponent and the vertical profile evolution of the aerosol to further examine the consistency of the SO2only and SO2+ash simulations against observations.

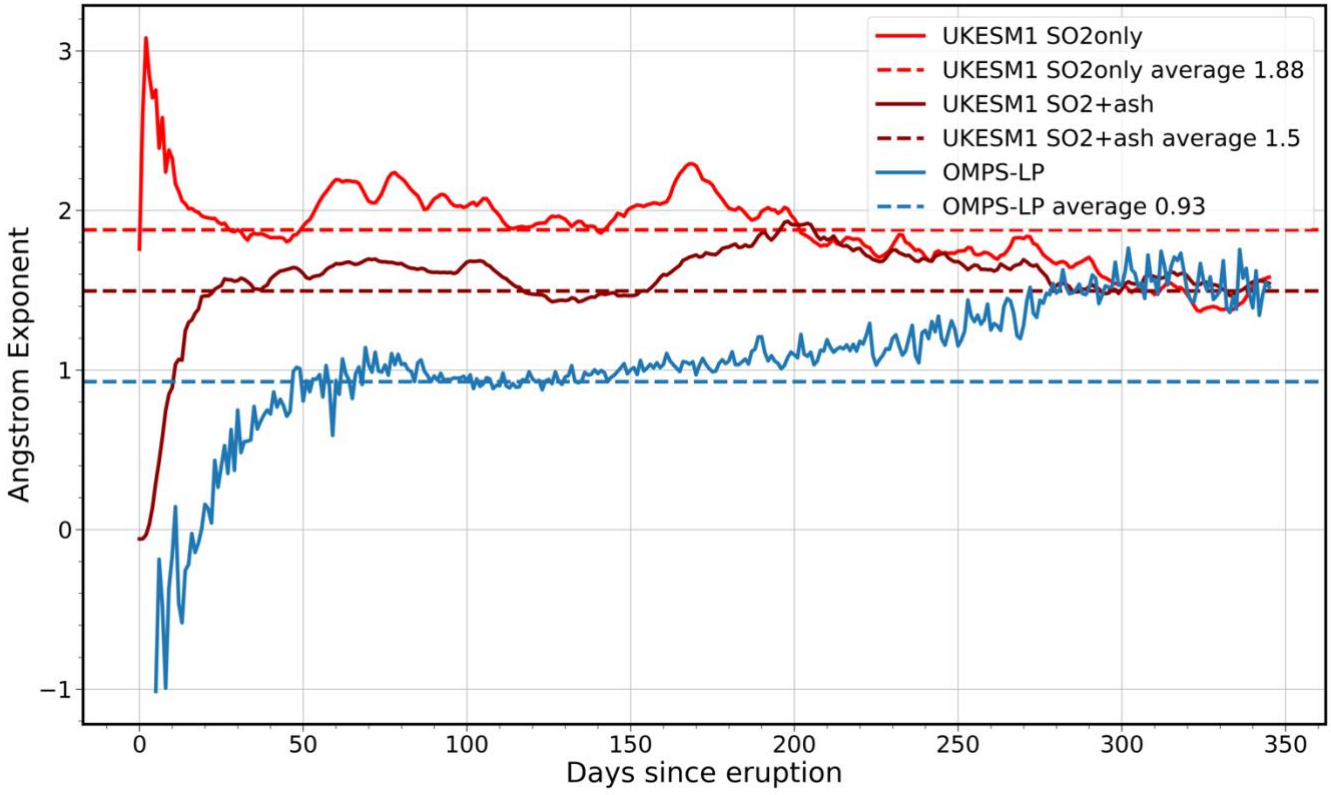

Figure 8: Daily evolution of Ångström Exponent for OMPS-LP (blue), UKESM1 SO2only (red) and UKESM1 SO2+ash (dark red). Calculated using area weighted sAOD between 30–90° N (same as Fig. 7) using 510nm and 869nm wavelengths.

4.5 Analysis of stratospheric aerosol Ångström Exponents

Without detailed in-situ measurements (e.g. Jégou et al., 2013) it is not possible to know with a high level of accuracy, the detailed size distribution of the volcanic aerosols. However, the wavelength dependence can be used to calculate the Ångström Exponent, since it is often used as an indicator of aerosol particle size. For measurements of optical depth τ_{λ_1} and τ_{λ_2} at wavelengths λ_1 and λ_2 the Ångström Exponent is given by Eq. (1):

$$\alpha = -\log\frac{\tau_{\lambda_1}}{\tau_{\lambda_2}} / \log\frac{\lambda_1}{\lambda_2}, \quad (1)$$

The OMPS-LP aerosol extinction measurements are provided at wavelengths ranging between 510 – 997nm, presenting the opportunity to calculate the sAOD and analyse the evolution of the Ångström Exponent and consequently variations in the

https://doi.org/10.5194/egusphere-2022-1060
Preprint. Discussion started: 26 October 2022

aerosol size distribution after the eruption. Figure 8 shows the daily Ångström Exponent (AE) for OMPS-LP, SO2only and SO2+ash calculated using the area averaged sAOD at wavelengths 510nm and 869nm between 30 – 90°N.

The observations show that the AE is initially close to between -1 and 0 indicating that large particles were observed immediately after the eruption, and therefore contains a significant amount of volcanic ash. After around 50 days after the eruption, the AE increases to approximately 1 for a period of over 3 months, this could suggest that the largest particles had dropped out and smaller particles remained. As the time after the eruption increases, the AE increases to a maximum value of ~1.6. Kloss et al., 2021 estimate a pristine average AE of 1.7 using background sAODs which suggests that approximately 300 days after the eruption the observations have returned to pre-eruption AE average.

Both model simulations converge on an AE of around 1.6 after 300 days, however they both display starkly contrasting behaviour immediately after the eruption. In the SO2only scenario the initial AE is very high (up to around 3) indicating smaller particles and decreases with time. The behaviour of the AE is therefore the opposite of what is observed.

In comparison, during the first 10 days after the eruption, the SO2+ash scenario shows an AE of around zero initially owing to the presence of ash, which then increases as the ash falls out from the atmosphere. This behaviour is much more similar to what we see in the observations as compared to SO2only, confirming that our SO2+ash simulations are in better agreement with observations. However, the agreement is far from perfect with the model AE increasing much faster than what we see in the observations, it then converges with the SO2only scenario approximately 200 days after the eruption. This figure again suggests that the SO2+ash scenario is better at representing the observations compared to the SO2only case. Further discussion of this is provided in Sect. 5.

4.6 Aerosol extinction vertical profile analysis

Figure 9 shows the vertical evolution of the CALIOP derived aerosol extinction coefficient with monthly averages and standard deviation from July until December. We also include both model simulations, SO2only (dashed red line) and SO2+ash (solid red line) for comparison. The observed monthly tropopause height (mean and standard deviation) is also included to highlight tropospheric and stratospheric altitudes. Both observations and model simulations are averaged over 30 – 90°N, not including those latitudes where CALIOP night retrievals are unable to retrieve data due to polar summer. Since CALIOP aerosol extinction retrievals have a minimum detection threshold of 0.012 km^{-1} (Toth et al., 2018) this limit has also been applied to the SO2only and SO2+ash data for a more consistent comparison. In the CALIOP observations we can see that initially after the eruption there are two peaks at ~11km and ~14.5km similar to the two injection altitudes used to initialise the UKESM1 simulations. The observations then form a singular peak above the tropopause at ~14km which increases in magnitude until a peak of 5.3 x 10^{-3} km^{-1} between September and October. After this, the observations show much of the aerosol plume below the average tropopause height and by December the magnitude of aerosol extinction coefficient is negligible. The vertical

https://doi.org/10.5194/egusphere-2022-1060
Preprint. Discussion started: 26 October 2022

profile analysis of the CALIOP aerosol extinction coefficient indicates how close the volcanic plume was to the tropopause in the first month or so after the eruption. This could explain why the OMPS-LP dataset missed the initial sAOD peak since limb-instruments can fail to detect aerosol near the tropopause (e.g. Fromm et al., 2014).

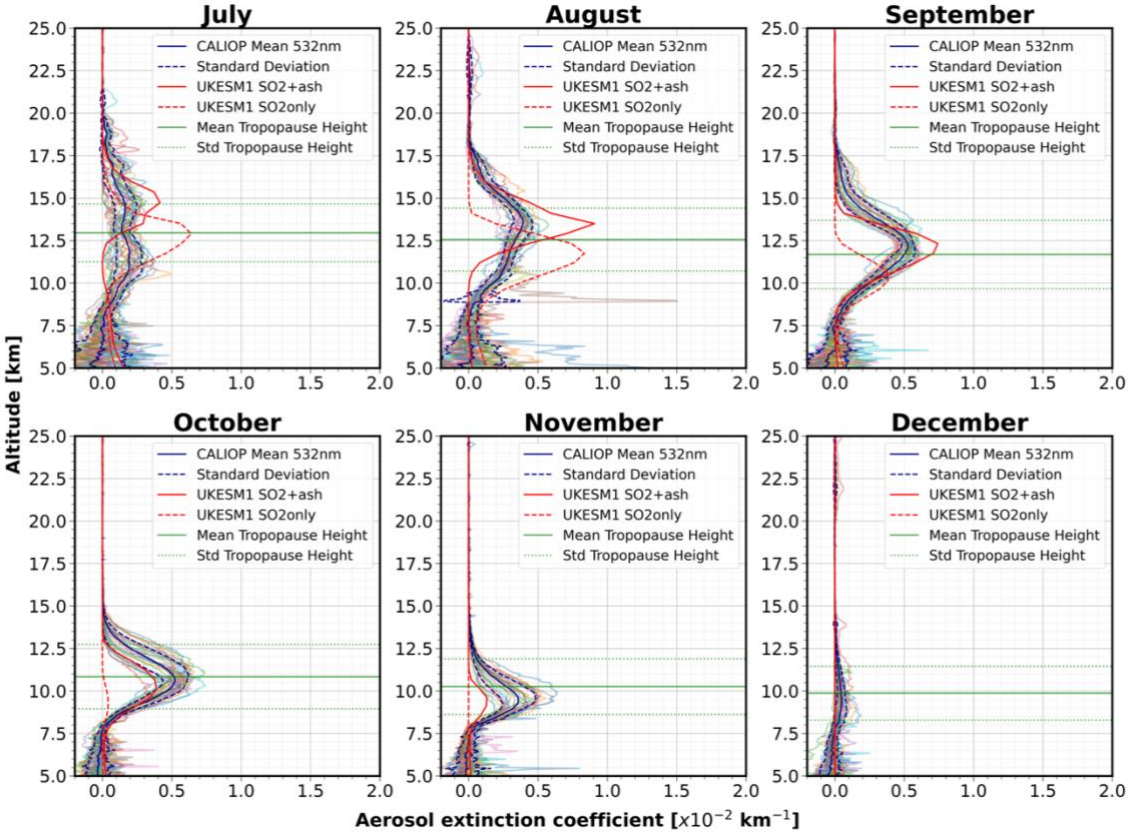

Figure 9: Aerosol extinction coefficient vertical profile averaged over 30–90° N. Averaged daily CALIOP aerosol extinction coefficient vertical profiles (night retrievals only, fainter lines) with monthly average (bold blue) and monthly average plus/minus standard deviation (solid dashed black lines). UKESM1 SO2+ash (solid bold red) and SO2 only (dashed bold red) simulations with imposed CALIOP minimum retrieval limits and mask. Average tropopause height is shown by the horizontal green line and the average tropopause height +/- one standard deviation for 2019 is also shown in green dotted lines.

In comparison, both model simulations peak in August, 8.3 x 10^{-3} km^{-1} for SO2only and 9.1 x 10^{-3} km^{-1} for SO2+ash almost 2 months prior to that seen in the observations. This could be due to aerosol microphysical processes such as the rate of coagulation and/or condensation or how the model represents new particle formation. In cases where SO_2 concentrations are high, such as Pinatubo, the conversion of H_2SO_4 produces large numbers of new aerosol particles and the rate of coagulation is high (Thomason, 1992). This results in a rapid increase of aerosol extinction as the aerosols

https://doi.org/10.5194/egusphere-2022-1060
Preprint. Discussion started: 26 October 2022

grow. However, when there are fewer new aerosol particles, after a more modest eruption for example, the rate of coagulation is slower. Since small particles, particularly those with radii smaller than 0.1μm, are poor scatterers of solar radiation the initial optical signal can be reduced until the particles grow to a larger size. In this case the observations seem to reflect the latter scenario with a more delayed peak in aerosol extinction, whereas both models suggest the former. We notice that in the model simulations the accumulation mode increases quickly, dominating the column aerosol burden, with very little in the nucleation mode. This could explain the earlier and larger peaks in the model compared to the observations, since aerosols in the accumulation mode produce a greater optical signal.

There is also a significant difference between the two model scenarios. In July the peak aerosol extinction for SO2only is at approximately 13km, a similar altitude to the average tropopause height. In contrast to this, the SO2+ash plume has a peak aerosol extinction at ~15km. This initial difference in height results in a significant impact on the lifetime of the aerosol. In the SO2+ash scenario the aerosol plume resides mostly in the stratosphere until October where the peak is just below the average tropopause height, whereas the SO2only plume is mostly beneath the average tropopause height as early as August. Due to more removal processes in the troposphere this results in a much faster decay rate and shorter lifetime. Since both model scenarios were initialised with the same SO_2 injection altitudes the difference between plume altitudes in July must be due to the self-lofting effect from the ash. Muser et al., 2020 observed this after the Raikoke eruption and noted that the maximum cloud-top height rose more than 6km within the first few days after the eruption. Whilst the SO2+ash scenario overestimates the magnitude of the aerosol extinction coefficient in the first few months, it does represent the altitude and lifetime of the aerosol plume well.

The additional analysis of aerosol size evolution and vertical profile have confirmed that the UKESM1 SO2+ash simulation is more consistent with the observations. Figs. 8 and 9 illustrate that SO2+ash provides a much better representation of the aerosol size and lifetime and therefore resulting climatic impact than the SO2only scenario.

4.7 Radiative impact

Haywood et al., 2010 explored the difference between the aerosol optical depth and radiative impact due to anthropogenic aerosol and the Sarychev Peak stratospheric aerosol plume. They found that in some regions of the NH the AOD was of comparable magnitude or greater than the AOD from anthropogenic emissions. In Figure 10 we have recreated the Sarychev Peak AOD and radiative impact plots from Haywood et al., 2010 Figure 12 using data from HadGEM2 and compare them against the UKESM1 SO2+ash Raikoke simulation. The cloud-free radiative impact was calculated in the same manner as Haywood et al., 2010 using the following equation, Eq. (2):

$$Radiative\ impact\ \approx (SW_{CTL} - SW_{EXP}) * (1 - A_c), \quad (2)$$

https://doi.org/10.5194/egusphere-2022-1060
Preprint. Discussion started: 26 October 2022

where SW is the clear-sky outgoing shortwave radiation (Wm^{-2}) at the top of the atmosphere (TOA) for the control (CTL) and experiment (EXP) and A_c is the cloud fraction (Haywood et al., 1997).

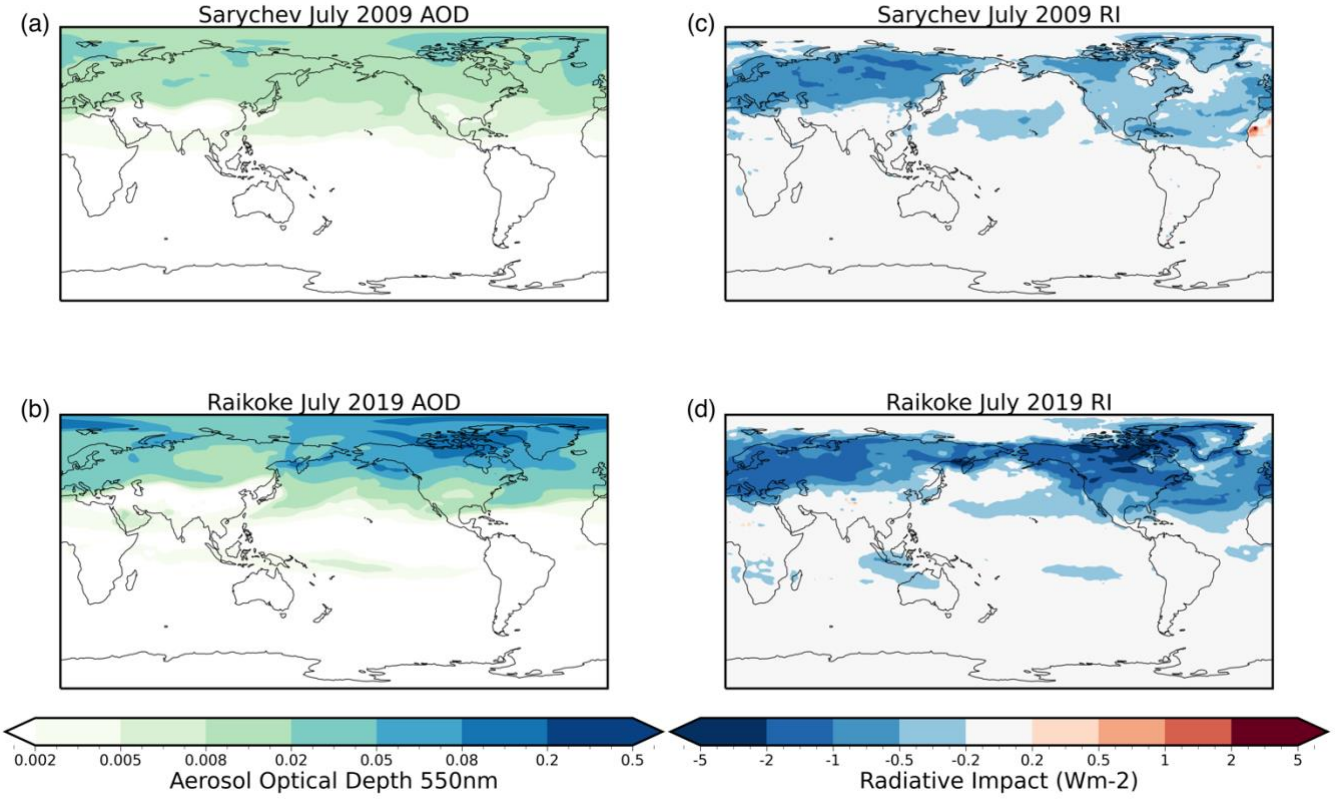

Figure 10: The sAOD for July at 550nm for a) Sarychev Peak derived from HadGEM2 and b) Raikoke derived from UKESM1. The cloud-free radiative impact at the top of the atmosphere (Wm^{-2}) for c) Sarychev Peak derived from HadGEM2 and d) Raikoke derived from UKESM1.

	Global	Northern Hemisphere	Southern Hemisphere
Sarychev Peak	− 0.14	− 0.27	− 0.004
Raikoke	− 0.28	− 0.52	− 0.05

Table 2: The cloud-free radiative impact (in Wm^{-2}) at the top of the atmosphere calculated globally, for the Northern Hemisphere and the Southern Hemisphere for Sarychev Peak derived from HadGEM2 and for Raikoke derived from UKESM1.

https://doi.org/10.5194/egusphere-2022-1060
Preprint. Discussion started: 26 October 2022

Both plots show that the Raikoke eruption had a greater impact on the global AOD and a larger cloud-free radiative impact. The NH average AOD after the Sarychev Peak eruption was approximately 0.01 compared to 0.03 after the Raikoke eruption. We also note that we cannot make exact global comparisons between our analysis and the Sarychev Peak eruption due to the impacts of the first Ulawun eruption (26th June) in UKESM1 which can be observed in both plots just south of the Equator in the Pacific. The cloud-free radiative impact from the Raikoke eruption in comparison to the Sarychev Peak eruption is substantially greater (Table 2). In the NH the cloud-free radiative impact of Raikoke is -0.52 Wm^{-2}, almost double that of Sarychev Peak (-0.27 Wm^{-2}). The cooling effect is greatest over North America, similar to the distribution of sAOD. This is in contrast to the Sarychev Peak eruption, where the modelled radiative impact indicated a stronger cooling over Russia in comparison to North America.

5. Discussion and conclusion

This study provides a comprehensive analysis of satellite and ground-based observational data to determine if including ash in model simulations of volcanic eruptions can more accurately represent aerosol size, geographic distribution, and the evolution of volcanic plumes. There are substantial differences between observations due to different observational limitations. Whilst these were difficult to reconcile, we were able to apply numerous observational thresholds to UKESM1 to assess the ability of the model to replicate observations. Using multiple remote sensing methods we were able to validate the transport of the SO_2 plume, the evolution of the sulfate aerosol and associated radiative impacts modelled by the UKESM1 nudged to ERA5 reanalysis data.

The Raikoke eruption was the largest volcanic injection of SO_2 into the stratosphere since the OMPS satellite was launched and was well observed by OMPS-NM. This revealed that the plume became trapped within a cyclonic circulation for several days across Eastern Russia and Alaska before travelling eastwards across North America and the North Atlantic. This agrees with other satellite observations used in previous studies (e.g., Kloss et al., 2021, Vaughan et al., 2020). When nudged to ERA5 reanalysis data the UKESM1 SO2only and SO2+ash simulations were able to represent the position of the main features of the plume evolution, including the cyclonic circulation. It is worth noting that despite injecting the estimated observed 1.5 Tg SO_2 the observations saw a peak SO_2 column burden in this area of 0.76 DU, almost double that seen in the model. Increasing the amount of SO_2 injected into the model simulations would have ameliorated this difference, however, this would lead to a significant overestimate of sulfate aerosol and sAOD, which would not have agreed with observations.

The distribution of the sulfate aerosol plume was examined using two satellite observations with comparisons to the UKESM1 model simulations. The zonal evolution observed by CALIOP, and OMPS-LP followed a similar geographic evolution to the Sarychev Peak eruption in June 2009 (Haywood et al., 2010) which was to be expected since they are neighbouring volcanoes and the altitude and injection magnitude of Sarychev Peak (11 – 15km, 1.2 $\pm$ 0.2 Tg) were similar to that of Raikoke (10 –

https://doi.org/10.5194/egusphere-2022-1060
Preprint. Discussion started: 26 October 2022

15km, 1.5 ± 0.2 Tg). Due to differences in minimum detection thresholds it was observed that the CALIOP data did not represent the long-term evolution of the sulfate aerosol plume well and similarly to other limb-instruments, OMPS-LP can fail to detect aerosol near the tropopause at the beginning of an eruption. Hence, we created a combined dataset consisting of both CALIOP and OMPS-LP aerosol extinction data. Data from the Mauna Loa Observatory provided additional corroborative evidence that the OMPS-LP observations were more appropriate after the plume had dispersed, with CALIOP observations showing no significant increase in sAOD for the eruption year. Model simulations differed in the MLO region, with the SO2+ash case presenting similar values of sAOD to both the OMPS-LP and AERONET observations. In contrast, the SO2only simulation revealed values of sAOD much lower than those seen in the observations and SO2+ash case.

We then studied the observed Ångström Exponent utilising the OMPS-LP 869nm and 510nm wavelength aerosol extinction coefficient retrievals. Throughout the first 50 days after the eruption the AE was less than one, indicating the presence of large aerosol particles. Comparing the observations to both the SO2only and SO2+ash UKESM1 scenario demonstrates that whilst both models do not capture the observations completely, the SO2+ash scenario better represents the change in aerosol size after the eruption. It is also an indicator that the model removes the ash much faster than we see in the observations. Zhu et al., 2020 proposed that after the 2014 Mount Kelud eruption the volcanic aerosol layer was primarily composed of low density, super-micron sized ash. Most model simulations assume volcanic ash particles are denser than the pumice-like particles observed in Zhu et al. (2020) and hence the ash particles in model simulations fall out more quickly. This could explain the difference between the observations and the SO2+ash model case. Obviously, there are limitations to our assumption that the ash is externally mixed with the sulfate aerosol as in reality there will be varying degrees of internal and external mixture.

It is possible that the observations were also influenced by the Siberian wildfires which occurred in July and August 2019. The wildfires were extreme and lasted from 19th July to 14th August 2019 (between 28-54 days after the eruption; Johnson et al., 2019) injecting wildfire smoke into the troposphere near to the Arctic region. Ohneiser et al., 2021 suggested that the influence from the Siberian wildfire smoke increased the aerosol optical depth across the Arctic region. Whilst there might have been some influence on the aerosol optical properties and distribution from this event, our simulations suggest that the SO2+ash model provides a reasonable representation of the Raikoke eruption without including the Siberian wildfires in the model simulation.

We utilised the CALIOP aerosol extinction coefficient night-time retrievals to examine the evolution of the vertical profile of the plume. We initially observed two distinct peaks just above and just below the average tropopause height before a singular peak at around 14km was observed from August onwards. The SO2+ash model represents the altitude of the aerosol well throughout the months following the eruption, however the SO2only simulation displayed values of aerosol extinction consistently lower in altitude resulting in a much faster decay rate due to transfer to the troposphere through tropospheric folds. The modelled aerosol extinction peak was prematurely early and overestimated in both scenarios which could be due to the

https://doi.org/10.5194/egusphere-2022-1060
Preprint. Discussion started: 26 October 2022

rate of coagulation in the stratosphere or how the model represents new particle formation. After more moderate volcanic eruptions the rate of coagulation can be slower resulting in smaller less optically active particles and a delayed aerosol extinction peak. We see in both model simulations the accumulation mode dominates the column aerosol burden. This suggests that the rate of transfer from optically inactive Aitken to optically active accumulation mode in the model may be too fast.

Finally the impact of the modelled Raikoke eruption was compared to the HadGEM2 simulation of the Sarychev Peak eruption. The Northern Hemisphere mean perturbation to the sAOD during July after the Sarychev Peak eruption was 0.01 compared to 0.028 after the Raikoke eruption. In July the UKESM1 simulation also included the first Ulawun eruption, causing a perturbed sAOD in the Southern Hemisphere of 0.0004. The radiative impact of the Raikoke eruption in July on the Northern Hemisphere was -0.51 Wm^{-2} almost double that seen in the July after the Sarychev Peak eruption, -0.27 Wm^{-2}, despite only a 25% increase in the injected SO_2 amount. Whilst the eruptions were similar in altitude and latitude, the impact seen in UKESM1 is far greater in Raikoke than after Sarychev Peak. Some of these differences may stem from the large dependence on meteorology that has been noted for low-altitude eruptions (Jones et al., 2016).

Accurately modelling the evolution of volcanic plumes and therefore identifying the impacts they have on the climate is a difficult task. Our analysis provides several lines of evidence to suggest that including ash in model emission schemes can improve the representation of volcanic plumes in global climate models. Whilst the model is not perfect at representing each process it provides reasonable *e*-folding times for the conversion of SO_2 to sulfate aerosol and models the geographic distribution of the aerosol well. Future work might consider internal mixture of sulfate and ash aerosol which could yield differences in the aerosol microphysical and optical properties. A better representation of volcanic ash could also be applied, since this study used mineral dust as a proxy since the refractive indices and size distributions are similar. Ultimately, this study has shown that volcanic emissions are far more complicated than simple injections of SO_2 and that limitations in remote sensing observations hamper definitive attribution of particle composition. These results suggest the strong need for in situ sampling of aerosol from instrumentation on airborne observational platforms. While such measurements of ash-sulfate mixtures have been performed following eruptions that predominantly loaded the troposphere (e.g. Johnson et al., 2021; Turnbull et al., 2012; Newman et al., 2013), the dearth of such measurements in the stratosphere means that definitive attribution of aerosol composition, and microphysical and optical properties remains extremely challenging.

https://doi.org/10.5194/egusphere-2022-1060
Preprint. Discussion started: 26 October 2022

Author Contributions

AW, MO and LDP analysed the satellite and in-situ data and created the combined observational dataset. AJ and JH devised the experimental set up for UKESM1. AW, AJ and JH analysed the results of the simulations. AW prepared the manuscript with contributions from all co-authors.

Competing interests

The authors declare that they have no conflict of interest.

Acknowledgements

AW was funded via a UKRI Centre for Doctoral Training in Environmental Intelligence PhD studentship hosted by the University of Exeter. JH, AJ, MO was supported by the Met Office Hadley Centre Climate Programme funded by BEIS. JH would also like to acknowledge support from the NERC funded EXTEND project (NE/W003880/1) and from SilverLining through its Safe Climate Research Initiative. LDP was supported from the NERC funded SASSO standard grant (NE/S00212X/1). JH and DP would like to acknowledge the support of the NERC funded ADVANCE project (NE/T006897/1).

References

Archibald, A. T., O'Connor, F. M., Abraham, N. L., Archer-Nicholls, S., Chipperfield, M. P., Dalvi, M., Folberth, G. A., Dennison, F., Dhomse, S. S., Griffiths, P. T., Hardacre, C., Hewitt, A. J., Hill, R. S., Johnson, C. E., Keeble, J., Köhler, M. O., Morgenstern, O., Mulcahy, J. P., Ordóñez, C., Pope, R. J., Rumbold, S. T., Russo, M. R., Savage, N. H., Sellar, A., Stringer, M., Turnock, S. T., Wild, O., and Zeng, G.: Description and evaluation of the UKCA stratosphere–troposphere chemistry scheme (StratTrop vn 1.0) implemented in UKESM1, Geoscientific Model Development, 13, 1223-1266, 10.5194/gmd-13-1223-2020, 2020.

Barnes, J. E. and Hofmann, D. J.: Lidar measurements of stratospheric aerosol over Mauna Loa Observatory, Geophysical Research Letters, 24, 1923-1926, 10.1029/97gl01943, 1997.

Bluth, G. J. S., Doiron, S. D., Schnetzler, C. C., Krueger, A. J., and Walter, L. S.: Global Tracking of the SO2 Clouds from the June 1991 Mount Pinatubo Eruptions, Geophysical Research Letters, 19, 151-154, 1992.

Bruckert, J., Hoshyaripour, G. A., Horváth, Á., Muser, L. O., Prata, F. J., Hoose, C., and Vogel, B.: Online treatment of eruption dynamics improves the volcanic ash and SO₂ dispersion forecast: case of the 2019 Raikoke eruption, Atmospheric Chemistry and Physics, 22, 3535-3552, 10.5194/acp-22-3535-2022, 2022.

Chouza, F., Leblanc, T., Barnes, J., Brewer, M., Wang, P., and Koon, D.: Long-term (1999–2019) variability of stratospheric aerosol over Mauna Loa, Hawaii, as seen by two co-located lidars and satellite measurements, Atmos. Chem. Phys., 20, 6821-6839, 10.5194/acp-20-6821-2020, 2020.

https://doi.org/10.5194/egusphere-2022-1060
Preprint. Discussion started: 26 October 2022

Clarisse, L., Hurtmans, D., Clerbaux, C., Hadji-Lazaro, J., Ngadi, Y., and Coheur, P. F.: Retrieval of sulphur dioxide from the infrared atmospheric sounding interferometer (IASI), Atmospheric Measurement Techniques, 5, 581-594, 10.5194/amt-5-581-2012, 2012.

de Leeuw, J., Schmidt, A., Witham, C. S., Theys, N., Taylor, I. A., Grainger, R. G., Pope, R. J., Haywood, J., Osborne, M., and Kristiansen, N. I.: The 2019 Raikoke volcanic eruption – Part 1: Dispersion model simulations and satellite retrievals of volcanic sulfur dioxide, Atmospheric Chemistry and Physics, 21, 10851-10879, 10.5194/acp-21-10851-2021, 2021.

Dhomse, S. S., Emmerson, K. M., Mann, G. W., Bellouin, N., Carslaw, K. S., Chipperfield, M. P., Hommel, R., Abraham, N. L., Telford, P., Braesicke, P., Dalvi, M., Johnson, C. E., O'Connor, F., Morgenstern, O., Pyle, J. A., Deshler, T., Zawodny, J. M., and Thomason, L. W.: Aerosol microphysics simulations of the Mt.~Pinatubo eruption with the UM-UKCA composition-climate model, Atmospheric Chemistry and Physics, 14, 11221-11246, 10.5194/acp-14-11221-2014, 2014.

Edwards, J. and Slingo, A.: Studies with a flexible new radiation code. I: Choosing a configuration for a large-scale model, Quarterly Journal of the Royal Meteorological Society, 122, 689-719, 1996.

Fromm, M., Kablick, G., Nedoluha, G., Carboni, E., Grainger, R., Campbell, J., and Lewis, J.: Correcting the record of volcanic stratospheric aerosol impact: Nabro and Sarychev Peak, Journal of Geophysical Research: Atmospheres, 119, 10,343-310,364, 10.1002/2014jd021507, 2014.

Gordeev, E. I. and Girina, O. A.: Volcanoes and their hazard to aviation, Herald of the Russian Academy of Sciences, 84, 1-8, 10.1134/s1019331614010079, 2014.

Gorkavyi, N., Krotkov, N., Li, C., Lait, L., Colarco, P., Carn, S., DeLand, M., Newman, P., Schoeberl, M., Taha, G., Torres, O., Vasilkov, A., and Joiner, J.: Tracking aerosols and SO₂ clouds from the Raikoke eruption: 3D view from satellite observations, Atmospheric Measurement Techniques, 14, 7545-7563, 10.5194/amt-14-7545-2021, 2021.

Guo, S., Bluth, G. J. S., Rose, W. I., Watson, I. M., and Prata, A. J.: Re-evaluation of SO2release of the 15 June 1991 Pinatubo eruption using ultraviolet and infrared satellite sensors, Geochemistry, Geophysics, Geosystems, 5, n/a-n/a, 10.1029/2003gc000654, 2004.

Haynes, P.: STRATOSPHERIC DYNAMICS, Annual Review of Fluid Mechanics, 37, 263-293, 10.1146/annurev.fluid.37.061903.175710, 2005.

Haywood, J. M., Jones, A., Clarisse, L., Bourassa, A., Barnes, J., Telford, P., Bellouin, N., Boucher, O., Agnew, P., Clerbaux, C., Coheur, P., Degenstein, D., and Braesicke, P.: Observations of the eruption of the Sarychev volcano and simulations using the HadGEM2 climate model, Journal of Geophysical Research, 115, 10.1029/2010jd014447, 2010.

Haywood, J. M., Jones, A., and Jones, G. S.: The impact of volcanic eruptions in the period 2000-2013 on global mean temperature trends evaluated in the HadGEM2-ES climate model, Atmospheric Science Letters, 15, 92-96, 10.1002/asl2.471, 2014.

Hedelt, P., Efremenko, D. S., Loyola, D. G., Spurr, R., and Clarisse, L.: Sulfur dioxide layer height retrieval from Sentinel-5 Precursor/TROPOMI using FP_ILM, Atmospheric Measurement Techniques, 12, 5503-5517, 10.5194/amt-12-5503-2019, 2019.

https://doi.org/10.5194/egusphere-2022-1060
Preprint. Discussion started: 26 October 2022

Holben, B. N., Eck, T. F., Slutsker, I. a., Tanre, D., Buis, J., Setzer, A., Vermote, E., Reagan, J. A., Kaufman, Y., and Nakajima, T.: AERONET—A federated instrument network and data archive for aerosol characterization, Remote sensing of environment, 66, 1-16, 1998.

Jégou, F., Berthet, G., Brogniez, C., Renard, J. B., François, P., Haywood, J. M., Jones, A., Bourgeois, Q., Lurton, T., Auriol, F., Godin-Beekmann, S., Guimbaud, C., Krysztofiak, G., Gaubicher, B., Chartier, M., Clarisse, L., Clerbaux, C., Balois, J. Y., Verwaerde, C., and Daugeron, D.: Stratospheric aerosols from the Sarychev volcano eruption in the 2009 Arctic summer, Atmos. Chem. Phys., 13, 6533-6552, 10.5194/acp-13-6533-2013, 2013.

Johnson, B., Turnbull, K., Brown, P., Burgess, R., Dorsey, J., Baran, A. J., Webster, H., Haywood, J., Cotton, R., Ulanowski, Z., Hesse, E., Woolley, A., and Rosenberg, P.: In situ observations of volcanic ash clouds from the FAAM aircraft during the eruption of Eyjafjallajökull in 2010, Journal of Geophysical Research: Atmospheres, 117, 10.1029/2011jd016760, 2012.

Johnson, B., Turnbull, K., Brown, P., Burgess, R., Dorsey, J., Baran, A. J., Webster, H., Haywood, J., Cotton, R., Ulanowski, Z., Hesse, E., Woolley, A., and Rosenberg, P.: In situ observations of volcanic ash clouds from the FAAM aircraft during the eruption of Eyjafjallajökull in 2010, Journal of Geophysical Research: Atmospheres, 117, https://doi.org/10.1029/2011JD016760, 2012.

Johnson, J., Taha, G., Loughman, R., Zhu, T., and DeLand, M.: README Document for the Suomi-NPP OMPS LP L2 AER Daily Product, 2020.

Johnson, M. S., Strawbridge, K., Knowland, K. E., Keller, C., and Travis, M.: Long-range transport of Siberian biomass burning emissions to North America during FIREX-AQ, Atmospheric Environment, 252, 10.1016/j.atmosenv.2021.118241, 2021.

Jones, A. C., Haywood, J. M., Jones, A., and Aquila, V.: Sensitivity of volcanic aerosol dispersion to meteorological conditions: A Pinatubo case study, Journal of Geophysical Research: Atmospheres, 121, 6892-6908, https://doi.org/10.1002/2016JD025001, 2016.

Jones, A. C., Haywood, J. M., Dunstone, N., Emanuel, K., Hawcroft, M. K., Hodges, K. I., and Jones, A.: Impacts of hemispheric solar geoengineering on tropical cyclone frequency, Nat Commun, 8, 1382, 10.1038/s41467-017-01606-0, 2017.

Karagulian, F., Clarisse, L., Clerbaux, C., Prata, A. J., Hurtmans, D., and Coheur, P. F.: Detection of volcanic SO2, ash, and H2SO4using the Infrared Atmospheric Sounding Interferometer (IASI), Journal of Geophysical Research, 115, 10.1029/2009jd012786, 2010.

Kloss, C., Berthet, G., Sellitto, P., Ploeger, F., Taha, G., Tidiga, M., Eremenko, M., Bossolasco, A., Jégou, F., Renard, J.-B., and Legras, B.: Stratospheric aerosol layer perturbation caused by the 2019 Raikoke and Ulawun eruptions and their radiative forcing, Atmospheric Chemistry and Physics, 21, 535-560, 10.5194/acp-21-535-2021, 2021.

Kravitz, B., Robock, A., and Bourassa, A.: Negligible climatic effects from the 2008 Okmok and Kasatochi volcanic eruptions, Journal of Geophysical Research, 115, 10.1029/2009jd013525, 2010.

Langmann, B.: On the Role of Climate Forcing by Volcanic Sulphate and Volcanic Ash, Advances in Meteorology, 2014, 1-17, 10.1155/2014/340123, 2014.

https://doi.org/10.5194/egusphere-2022-1060
Preprint. Discussion started: 26 October 2022

Lawrence, M. G., Schäfer, S., Muri, H., Scott, V., Oschlies, A., Vaughan, N. E., Boucher, O., Schmidt, H., Haywood, J., and Scheffran, J.: Evaluating climate geoengineering proposals in the context of the Paris Agreement temperature goals, Nature communications, 9, 1-19, 2018.

Mann, G. W., Carslaw, K. S., Spracklen, D. V., Ridley, D. A., Manktelow, P. T., Chipperfield, M. P., Pickering, S. J., and Johnson, C. E.: Description and evaluation of GLOMAP-mode: a modal global aerosol microphysics model for the UKCA composition-climate model, Geoscientific Model Development, 3, 519-551, 10.5194/gmd-3-519-2010, 2010.

McCormick, P. M., Thomason, L., and Trepte, C.: Atmospheric effecrs of the Mt Pinatubo eruption, Nature, 373, 1995.

Millington, S. C., Saunders, R. W., Francis, P. N., and Webster, H. N.: Simulated volcanic ash imagery: A method to compare NAME ash concentration forecasts with SEVIRI imagery for the Eyjafjallajökull eruption in 2010, Journal of Geophysical Research: Atmospheres, 117, https://doi.org/10.1029/2011JD016770, 2012.

Muser, L. O., Hoshyaripour, G. A., Bruckert, J., Horváth, Á., Malinina, E., Wallis, S., Prata, F. J., Rozanov, A., von Savigny, C., Vogel, H., and Vogel, B.: Particle aging and aerosol–radiation interaction affect volcanic plume dispersion: evidence from the Raikoke 2019 eruption, Atmospheric Chemistry and Physics, 20, 15015-15036, 10.5194/acp-20-15015-2020, 2020.

Newman, S. M., Clarisse, L., Hurtmans, D., Marenco, F., Johnson, B., Turnbull, K., Havemann, S., Baran, A. J., O'Sullivan, D., and Haywood, J.: A case study of observations of volcanic ash from the Eyjafjallajökull eruption: 2. Airborne and satellite radiative measurements, Journal of Geophysical Research: Atmospheres, 117, https://doi.org/10.1029/2011JD016780, 2012.

Niemeier, U., Timmreck, C., Graf, H.-F., Kinne, S., Rast, S., and S., S.: Initial fate of fine ash and sulfur from large volcanic eruptions, Atmospheric Chemistry and Physics, 2009.

Ohneiser, K., Ansmann, A., Chudnovsky, A., Engelmann, R., Ritter, C., Veselovskii, I., Baars, H., Gebauer, H., Griesche, H., Radenz, M., Hofer, J., Althausen, D., Dahlke, S., and Maturilli, M.: The unexpected smoke layer in the High Arctic winter stratosphere during MOSAiC 2019–2020, Atmospheric Chemistry and Physics, 21, 15783-15808, 10.5194/acp-21-15783-2021, 2021.

Osborne, M. J., de Leeuw, J., Witham, C., Schmidt, A., Beckett, F., Kristiansen, N., Buxmann, J., Saint, C., Welton, E. J., Fochesatto, J., Gomes, A. R., Bundke, U., Petzold, A., Marenco, F., and Haywood, J.: The 2019 Raikoke volcanic eruption – Part 2: Particle-phase dispersion and concurrent wildfire smoke emissions, Atmospheric Chemistry and Physics, 22, 2975-2997, 10.5194/acp-22-2975-2022, 2022.

Plumb, R. A.: A “tropical pipe” model of stratospheric transport, Journal of Geophysical Research: Atmospheres, 101, 3957-3972, https://doi.org/10.1029/95JD03002, 1996.

Ridley, J. K., Blockley, E. W., Keen, A. B., Rae, J. G. L., West, A. E., and Schroeder, D.: The sea ice model component of HadGEM3-GC3.1, Geoscientific Model Development, 11, 713-723, 10.5194/gmd-11-713-2018, 2018.

Robock, A.: Volcanic eruptions and climate, Reviews of Geophysics, 38, 191-219, 10.1029/1998rg000054, 2000.

Sellar, A. A., Jones, C. G., Mulcahy, J. P., Tang, Y., Yool, A., Wiltshire, A., O'Connor, F. M., Stringer, M., Hill, R., Palmieri, J., Woodward, S., Mora, L., Kuhlbrodt, T., Rumbold, S. T., Kelley, D. I., Ellis, R., Johnson, C. E., Walton, J., Abraham, N. L., Andrews, M. B., Andrews, T., Archibald, A. T., Berthou, S., Burke, E., Blockley, E., Carslaw, K., Dalvi, M., Edwards, J.,

https://doi.org/10.5194/egusphere-2022-1060
Preprint. Discussion started: 26 October 2022

Folberth, G. A., Gedney, N., Griffiths, P. T., Harper, A. B., Hendry, M. A., Hewitt, A. J., Johnson, B., Jones, A., Jones, C. D., Keeble, J., Liddicoat, S., Morgenstern, O., Parker, R. J., Predoi, V., Robertson, E., Siahaan, A., Smith, R. S., Swaminathan, R., Woodhouse, M. T., Zeng, G., and Zerroukat, M.: UKESM1: Description and Evaluation of the U.K. Earth System Model, Journal of Advances in Modeling Earth Systems, 11, 4513-4558, 10.1029/2019ms001739, 2019.

Shallcross, S.: The role of volcanic ash in the global dispersion of the aerosol cloud from major tropical eruptions, University of Leeds, 2020.

Shallcross, S., Mann, G., Schmidt, A., Haywood, J., Beckett, F., Jones, A., Neely, R., Vaughan, G., and Dhomse, S.: Long-lived ultra-fine ash particles within the Pinatubo volcanic aerosol cloud and their potential impact on its global dispersion and radiative forcings, April 01, 2021, 10.5194/egusphere-egu21-16034, 2021.

Storkey, D., Blaker, A. T., Mathiot, P., Megann, A., Aksenov, Y., Blockley, E. W., Calvert, D., Graham, T., Hewitt, H. T., Hyder, P., Kuhlbrodt, T., Rae, J. G. L., and Sinha, B.: UK Global Ocean GO6 and GO7: a traceable hierarchy of model resolutions, Geoscientific Model Development, 11, 3187-3213, 10.5194/gmd-11-3187-2018, 2018.

Taha, G.: OMPS-NPP L2 LP Aerosol Extinction Vertical Profile swath daily 3slit V2, Goddard Earth Sciences Data and Information Services Center (GES DISC) [dataset], 10.5067/CX2B9NW6FI27, 2020.

Taha, G., Loughman, R., Zhu, T., Thomason, L., Kar, J., Rieger, L., and Bourassa, A.: OMPS LP Version 2.0 multi-wavelength aerosol extinction coefficient retrieval algorithm, Atmospheric Measurement Techniques, 14, 1015-1036, 10.5194/amt-14-1015-2021, 2021.

Thomason, L.: Observations of a New SAGE II Aerosol Extinction Mode Following the Eruption of Mount Pinatubo, Geophysical Research Letters, 19, 1992.

Thomason, L. and Peter, T.: SPARC Assessment of Stratospheric Aerosol Properties (ASAP), 2006.

Toledano, C., González, R., Fuertes, D., Cuevas, E., Eck, T. F., Kazadzis, S., Kouremeti, N., Gröbner, J., Goloub, P., Blarel, L., Román, R., Barreto, Á., Berjón, A., Holben, B. N., and Cachorro, V. E.: Assessment of Sun photometer Langley calibration at the high-elevation sites Mauna Loa and Izaña, Atmos. Chem. Phys., 18, 14555-14567, 10.5194/acp-18-14555-2018, 2018.

Toth, T. D., Campbell, J. R., Reid, J. S., Tackett, J. L., Vaughan, M. A., Zhang, J., and Marquis, J. W.: Minimum aerosol layer detection sensitivities and their subsequent impacts on aerosol optical thickness retrievals in CALIPSO level 2 data products, Atmos Meas Tech, 11, 499-514, 10.5194/amt-11-499-2018, 2018.

Turnbull, K., Johnson, B., Marenco, F., Haywood, J., Minikin, A., Weinzierl, B., Schlager, H., Schumann, U., Leadbetter, S., and Woolley, A.: A case study of observations of volcanic ash from the Eyjafjallajökull eruption: 1. In situ airborne observations, Journal of Geophysical Research: Atmospheres, 117, 2012.

Vaughan, G., Wareing, D., and Ricketts, H.: Measurement Report: Lidar measurements of stratospheric aerosol following the 2019 Raikoke and Ulawun volcanic eruptions, Atmospheric Chemistry and Physics, 21, 5597-5604, 10.5194/acp-21-5597-2021, 2021.

https://doi.org/10.5194/egusphere-2022-1060
Preprint. Discussion started: 26 October 2022

Vernier, J. P., Fairlie, T. D., Deshler, T., Natarajan, M., Knepp, T., Foster, K., Wienhold, F. G., Bedka, K. M., Thomason, L., and Trepte, C.: In situ and space-based observations of the Kelud volcanic plume: The persistence of ash in the lower stratosphere, J Geophys Res Atmos, 121, 11104-11118, 10.1002/2016JD025344, 2016.

Winker, D. M., Powell, K. A., Hu, Y., Omar, A., Vaughan, M. A., Liu, Z., Hunt, W. H., and Young, S. A.: Overview of the CALIPSO Mission and CALIOP Data Processing Algorithms, Journal of Atmospheric and Oceanic Technology, 26, 2310-2323, 10.1175/2009jtecha1281.1, 2009.

Woodward, S.: Modeling the atmospheric life cycle and radiative impact of mineral dust in the Hadley Centre climate model, Journal of Geophysical Research: Atmospheres, 106, 18155-18166, 10.1029/2000jd900795, 2001.

Woodward, S.: Hadley Centre Technical Note 87 Mineral Dust in HadGEM 2 March 2011,

Woodward, S., Sellar, A., Tang, Y., Stringer, M., Yool, A., Robertson, E., and Wiltshire, A.: The simulation of mineral dust in the United Kingdom Earth System Model UKESM1., 10.5194/acp-2022-228, 2022.

Yang, K.: OMPS-NPP L2 NM Sulfur Dioxide (SO2) Total and Tropospheric Column swath orbital V2 [dataset], 10.5067/A9O02ZH0J94R, 2017.

Yool, A., Popova, E. E., and Anderson, T. R.: MEDUSA-2.0: an intermediate complexity biogeochemical model of the marine carbon cycle for climate change and ocean acidification studies, Geoscientific Model Development, 6, 1767-1811, 10.5194/gmd-6-1767-2013, 2013.

Zhu, Y., Toon, O. B., Jensen, E. J., Bardeen, C. G., Mills, M. J., Tolbert, M. A., Yu, P., and Woods, S.: Persisting volcanic ash particles impact stratospheric SO2 lifetime and aerosol optical properties, Nat Commun, 11, 4526, 10.1038/s41467-020-18352-5, 2020.